EUROPEAN ORGANISATION FOR NUCLEAR RESEARCH

CERN-EP / 87-190
October 6th 1987

# Search for New Heavy Quarks at the CERN Proton-Antiproton Collider.

*UA1 Collaboration, CERN, Geneva, Switzerland*

Aachen[1] - Amsterdam (NIKHEF)[2] - Annecy (LAPP)[3] - Birmingham[4] - CERN[5] - Harvard[6] - Helsinki[7] - Kiel[8] - Imperial College, London[9] - Queen Mary College, London[10] - Madrid (CIEMAT)[11] - MIT[12] - Padua[13] - Paris (College de France)[14] - Riverside[15] - Rome[16] - Rutherford Appleton Lab[17] - Saclay (CEN)[18] - Victoria[19] - Vienna[20] - Wisconsin[21] Collaboration

C. Albajar[5], M.G. Albrow[17], O.C. Allkofer[8], A. Astbury[19], B. Aubert[3], T. Axon[9], C. Bacci[16], T. Bacon[9], N. Bains[4], J. R. Batley[10], G. Bauer[6], S. Beingessner[19], J. Bellinger[21], A. Bettini[13], A. Bezaguet[5], R. Bonino[4], K. Bos[2], E. Buckley[10], G. Busetto[13], P. Catz[3], P. Cennini[5], S. Centro[13], F. Ceradini[16], D.G. Charlton[4], G. Ciapetti[16], S. Cittolin[5], D. Clarke[10], D. Cline[21], C. Cochet[18], J. Colas[3], P. Colas[18], M. Corden[4], J.A. Coughlan[17], G. Cox[4], D. Dau[8], M. DeBeer[18], J.P. deBrion[18], M. DeGiorgi[13], M. Della Negra[5], M. Demoulin[5], B. Denby[17], D. Denegri[18], A. DiCiaccio[5,16], F.J. Diez Hedo[11], L. Dobrzynski[14], J . Dorenbosch[2], J. D. Dowell[4,5], E. Duchovni[5], R. Edgecock[4], K. Eggert[1], E. Eisenhandler[10], N. Ellis[4], P. Erhard[1], H. Faissner[1], I.F. Fensome[10], A. Ferrando[11], M. Fincke-Keeler[19], P. Flynn[17], G. Fontaine[14], J. Garvey[4], D. Gee[15], S. Geer[6], A. Geiser[1], C. Ghesquiere[14], P. Ghez[3], C. Ghiglino[3], Y. Giraud-Heraud[14], A. Givernaud[18], A. Gonidec[5], H. Grassmann[1], G. Grayer[17], W. Haynes[17], S.J. Haywood[4], D.J. Holthuizen[2], A. Honma[10], M. Ikeda[15], W. Jank[5], M. Jimack[4], G. Jorat[5], P.I.P. Kalmus[10], V. Karimäki[7], R. Keeler[19], I. Kenyon[4], A. Kernan[15], A. Khan[9], W. Kienzle[5], R. Kinnunen[7], M. Krammer[20], J. Kroll[6], D. Kryn[14], F. Lacava[16], M. Landon[10], J. P. Laugier[18], J.P. Lees[3], R. Leuchs[8], S. Levegrün[8], S. Li[19], D. Linglin[3], E. Locci[5], K. Long[5], T. Markiewicz[21], C. Markou[9], M. Markytan[20], M.A. Marquina[11], G. Maurin[5], J.-P. Mendiburu[14], A. Meneguzzo[13], J. P. Merlo[15], T. Meyer[5], M.-N. Minard[3], M. Mohammadi[21], K. Morgan[15], M. Moricca[16], H.-G. Moser[1], B. Mours[3], Th. Muller[5], A. Nandi[10], L. Naumann[5], P. Nedelec[14], A. Nisati[16], A. Norton[5], F. Pauss[5], C. Perault[3], E. Petrolo[16], G. Piano Mortari[16], E. Pietarinen[7], C. Pigot[18], M. Pimiä[7], A. Placci[5], J.-P. Porte[5], M. Preischl[8], E. Radermacher[5], J. Ransdell[15], T. Redelberger[1], H. Reithler[1], J.-P. Revol[12], J. Richman[5], D. Robinson[9], T. Rodrigo[11], J. Rohlf[6], P. Rossi[13], C. Rubbia[5], W. Ruhm[5], G. Sajot[14], G. Salvini[16], J. Sass[5], D. Samyn[5], A. Savoy-Navarro[18], D. Schinzel[5], M. Schröder[8], A. Schwartz[6], W. Scott[17], C. Seez[9], T. P. Shah[17], I. Sheer[15], I. Siotis[9], D. Smith[15], R. Sobie[19], P. Sphicas[12], J. Strauss[20], J. Streets[4], C. Stubenrauch[18], D. Summers[21], K. Sumorok[6], F. Szoncso[20], C. Tao[14], A. Taurok[20], I. ten Have[2], S. Tether[12], G. Thompson[10], E. Tscheslog[1], J. Tuominiemi[7], A. van Dijk[2], B. van Eijk[2], J.P. Vialle[3], L. Villasenor[21], T.S. Virdee[9], H. von der Schmitt[5], W. von Schlippe[10], J. Vrana[14], V. Vuillemin[5], K. Wacker[1], G. Walzel[20], P. Watkins[4], A. Wildish[9], I. Wingerter[3], S. J. Wimpenny[5], X. Wu[12], C.-E. Wulz[5] , T. Wyatt[5], M. Yvert[3], C. Zaccardelli[16], I. Zacharov[2], N. Zaganidis[18], L. Zanello[16] and P. Zotto[13].

( Submitted to Zeitschrift für Physik C )

## ABSTRACT

We report on a search for new heavy quarks using data collected by the UA1 experiment during 1983, 1984 and 1985 at the CERN proton-antiproton collider, corresponding to an integrated luminosity of approximately 700 $nb^{-1}$.

Studying events with a muon or an isolated electron, accompanied by one or more jets, we find good agreement between our data and Monte Carlo predictions for the production of charm and beauty, without the need for a new quark. A top quark model, involving the decay $W \rightarrow t\bar{b}$ and direct $t\bar{t}$ production via the strong interaction, is used to determine our detection efficiency for top. This allows us to place an upper limit on the cross section for producing top quarks as a function of the top quark mass. Our analysis is not sensitive to the $W \rightarrow t\bar{b}$ process alone. By comparing our limit with a calculation of the $t\bar{t}$ cross section, added to the $W \rightarrow t\bar{b}$ cross section derived from our own measurements of $W \rightarrow \ell\nu$, we are able to place a lower limit on the mass of the top quark. From the lowest order ( $\alpha_s^2$) calculation, using the choice of structure functions and $Q^2$ scale that give the lowest cross section, we find:

$$m_{top} > 44 \text{ GeV}/c^2 \text{ (95\% c.l.)}$$

Including an estimate of the next higher order ($\alpha_s^3$) and calculating the cross section with the EUROJET QCD Monte Carlo program using a less extreme choice for the structure functions and $Q^2$ scale gives:

$$m_{top} > 56 \text{ GeV}/c^2 \text{ (95\% c.l.)}$$

A search has also been made for a fourth generation, charge 1/3 quark (b'). Assuming that the b' mass is smaller than that of the top quark and that it cannot be produced in W decays, the mass limits, using the above procedures, are respectively $m_{b'} > 32$ GeV/$c^2$ and $m_{b'} > 44$ GeV/$c^2$, both at 95% confidence level.

## 1.- INTRODUCTION

We report on a search for new heavy quarks using proton-antiproton collisions, at centre of mass energies of 546 and 630 GeV, recorded with the UA1 detector at the CERN collider. Two closely related searches have been performed, one for the top quark, the $SU(2)_L$ partner of the b quark, and the other for a fourth generation quark referred to here as the b' quark.

The existence of the top quark is an important open question. In the Standard Model with six quarks (u,d,s,c,b and t), flavour changing neutral currents are forbidden. On the other hand, if the top quark does not exist, the b quark must be a left handed iso-singlet, and processes such as b $\rightarrow$ (s or d) $\mu^+\mu^-$ cannot be avoided. The experimental limit $[(b \rightarrow \mu^+\mu^- X) / (b \rightarrow \text{all}) \leq 10^{-3}]$ [1] implies either that the top quark exists or that the Standard Model is not correct.

In the framework of the Standard Model, theoretical upper limits can be placed on the top quark mass [2] from the measurement of $\rho$, the parameter that specifies the relative strengths of the neutral and charged weak currents, and from a comparison of the measurements of $\sin^2(\theta_w)$ from UA1 and UA2 [3] with those at low $Q^2$. Thus, taking into account the recent lower limit from TRISTAN [4], the available evidence suggests that the top quark exists and that its mass lies in the range $26\ \text{GeV/c}^2 < m_{top} < 180\ \text{GeV/c}^2$. An indirect indication of a lower mass limit in the region of 50 GeV/$c^2$ has recently been obtained from analyses of $B^0$-$\bar{B}^0$ mixing [5]. For the b' quark, a lower mass limit of 22.7 GeV/$c^2$ at 95% confidence level has been measured at PETRA [6].

In 1984, we reported the first observation of events with an isolated, large transverse momentum electron or muon, together with two or more jets [7], based on our 1983 data (108 $\text{nb}^{-1}$) at $\sqrt{s}$ = 546 GeV. We raised the possibility that these events could be explained as the decay of a new heavy quark with a mass in the range 30 to 50 GeV/$c^2$. We have now increased the integrated luminosity by a factor of ~6 and have made further studies of the production of known heavy quarks (beauty and charm) using our muon data. Our improved understanding of the sources of lepton-jet events [8], which include heavy flavour decays, $W^{\pm}$, $Z^0$, Drell-Yan, $J/\psi$ and $\Upsilon$ production, allows us to obtain limits on the production of the top quark or any new heavy quark that decays semi-leptonically.

## 2.- CHARACTERISTICS OF HEAVY QUARK EVENTS

### *2.1) Semi-leptonic decays:*

In view of the large background of events containing high $p_T$ jets from QCD processes, the best way of identifying a new heavy quark is through its semi-leptonic decay modes, which typically have branching ratios of ~11%. The main sources of top quarks are W decay, where kinematically allowed, and direct QCD pair production. For the fourth generation b' quark, we assume that only the latter is possible.

*2.2 ) Lepton channels:*

The UA1 detector offers the possibility of searching for new heavy quarks in two independent channels, involving a prompt electron or a prompt muon respectively. Electrons and muons are identified using different parts of the apparatus and many of the systematic errors in the two cases are independent. It is shown later that the background sources to the prompt muon and electron signatures are also very different.

*2.3) Topology:*

In either channel, an event resulting from a heavy quark (top quark or b' quark ) decaying semi-leptonically will have a similar topology, namely an isolated lepton accompanied by two or more jets and a neutrino, all concentrated in the central pseudo-rapidity region ($|\eta| < 1.5$ ). These properties allow us to discriminate against other sources of charged leptons, $W^{\pm}$, $Z^{o}$, Drell-Yan, $J/\psi$, $\Upsilon$, $b\bar{b}$ and $c\bar{c}$, accompanied by gluons, that constitute the main physics backgrounds to a new heavy quark signal.

*2.3.a) Jets* --

Jets are defined in the calorimeters using the UA1 jet algorithm [9] and validated using the central detector information as described in [8]. A jet is counted if its axis lies outside a cone of radius $\Delta R \equiv (\Delta\eta^2+\Delta\phi^2)^{1/2} = 1$ around the lepton direction, where $\Delta\phi$ ($\Delta\eta$) is the difference in azimuthal angle (pseudo-rapidity) between the lepton and the jet axis, and $|\eta_{jet}| < 2.5$. Thus, a jet containing the charged lepton is not counted. Events are considered if they have at least one jet with $E_T > 12$ GeV, where $E_T$ is the uncorrected transverse energy of the jet as defined by the algorithm. Jet 1 is defined as the highest $E_T$ jet in the event. The other jets (if any), with $E_T > 7$ GeV, are numbered in order of decreasing $E_T$ and must be validated [8] by the presence of a charged track with $p_T > 0.5$ GeV/c and within $\Delta R = 0.4$ from the direction of the calorimeter jet axis. With this jet definition, an event coming from a semi-leptonic decay of a b or c quark will generally result in a topology with fewer jets than events coming from a top quark decay.

*2.3.b) Isolation of leptons* --

In the semi-leptonic decay of a new massive quark, the charged lepton will usually be emitted at a large angle with respect to the directions of the other decay products and will therefore tend to be isolated. Since the decays of beauty and charm quarks produce mainly non-isolated leptons, lepton isolation is a good way to discriminate between b, c and heavier quarks. As muons can be identified even if they are not isolated, they can be used to study the isolation properties of heavy flavour events [8]. In the UA1 detector, the activity around the charged lepton can be

measured in two independent ways, in the calorimeter ($\Sigma E_T$) and in the central track detector ($\Sigma p_T$) where either calorimeter cells or charged tracks within a cone of radius $\Delta R = 0.7$ around the lepton direction are considered. The transverse energy ($E_T$) and transverse momentum ($p_T$) are measured with respect to the beam axis. The size of the cone, $\Delta R$, is optimized taking into account the granularity of the detector and the fraction of energy from the underlying event (coming from the fragmentation of the spectator system and other jets in the event) contained in the cone. Since the acceptances of the calorimeter and of the central detector are different and complementary, it is important to use both pieces of information. We have therefore combined the two measurements into a single isolation variable : $I = ((\Sigma E_T/3)^2 + (\Sigma p_T/2)^2)^{1/2}$, where the relative weights are chosen to reflect the average values of these quantities for the underlying event, and $\Sigma E_T$ and $\Sigma p_T$ are expressed in GeV.

*2.3.c) Neutrinos --*

The neutrino transverse energy is estimated by the missing transverse energy in an event. Events in which the charged lepton-neutrino transverse mass, $m_T^{l\nu}$, exceeds 45 GeV/$c^2$ (electrons) or 40 GeV/$c^2$ (muons) are classified, for the purpose of this analysis, as W candidates. The transverse mass is defined as: $m_T^{l\nu} \equiv [2E_T^{l}E_T^{\nu}(1-\cos\Delta\phi_{l\nu})]^{1/2}$, where $E_T^{l}$ and $E_T^{\nu}$ are, respectively, the transverse energies of the charged lepton and of the neutrino, and $\Delta\phi_{l\nu}$ is the azimuthal angle difference between the charged lepton and the neutrino directions. The slightly different cuts reflect the different energy resolutions for electrons and muons.

*2.3.d) Dileptons --*

Events containing two prompt charged leptons, though less frequent, can also be used to search for evidence of heavy quarks. Events with a lepton pair ( $\mu\mu$, $\mu e$ or ee ) are considered.

## 3.- MONTE CARLO STUDIES

### *3.1) Event generation:*

A Monte Carlo program involving a full simulation of the detector response, acceptance and trigger efficiency is necessary to reproduce the expected features of the production and decay of a new heavy quark. In order to interpret the data, physics processes giving events with at least one muon or electron, accompanied by one or more jets, have been generated using the ISAJET QCD Monte Carlo program [10].

For $b\bar{b}$ and $c\bar{c}$ production, where the theoretical cross sections are not precisely known because of the incomplete inclusion of higher order terms (in $\alpha_s$) and because of uncertainties in the structure functions and fragmentation model, the inclusive muon-jet data have been used to normalize the Monte Carlo cross section [8]. In the case of Drell-Yan, J/$\Psi$ and $\Upsilon$ production, the

cross section has been normalized to our measurement of the dimuon cross section [11]. High $p_T$ Drell-Yan, J/Ψ and Υ pairs, accompanied by jets, are an important source of background for the new heavy quark search. However, our ability to measure their rate considerably reduces the associated uncertainty. The simulation of the above production mechanisms is discussed in [8].

For the top quark, the production mechanisms, fragmentation and decay modes considered have been chosen to conform with current theoretical expectations. Thus, the results presented here apply only to models in this class, described below. All events, generated with ISAJET [10], have been processed with full detector simulation, as discussed in [8].

*3.2) Top production mechanisms:*

The sources of top quarks considered are :

$$p\bar{p} \rightarrow W + X\,(W \rightarrow t\bar{b}) \qquad (1)$$

$$p\bar{p} \rightarrow Z + X\,(Z \rightarrow t\bar{t}) \qquad (2)$$

$$p\bar{p} \rightarrow t\bar{t} + X \qquad (3)$$

We take $m_W = 83$ GeV/$c^2$ and $m_Z = 93$ GeV/$c^2$. The production of a bound $t\bar{t}$ state (toponium), which has a comparatively negligible cross section, and diffractive production, for which there exists no definite theoretical prediction, have not been included.

*3.2.a) W and Z decays --*

For processes (1) and (2) the production cross sections are derived from our measurements of $W \rightarrow \ell\nu$ [12]. In the framework of the standard model the decays $W \rightarrow t\bar{b}$ and $Z \rightarrow t\bar{t}$ depend mainly on kinematics and, particularly for higher top masses, on QCD corrections to the partial decay widths [13].

*3.2.b) QCD cross sections --*

The cross section for process (3) can be estimated using perturbative QCD which should be more reliable than in the case of charm since the top mass is large. To lowest order in QCD, two subprocesses contribute: gluon fusion, $gg \rightarrow t\bar{t}$, and quark-antiquark annihilation, $q\bar{q} \rightarrow t\bar{t}$. For a top mass of 40 GeV/$c^2$, gluon fusion is expected to contribute 45% of the cross section; this falls to 25% for $m_{top} = 60$ GeV/$c^2$.

Three uncertainties affect the $O(\alpha_s^2)$ cross section estimate:

i) the uncertainty in the quark and gluon structure functions in the range $x \sim 0.05$–$0.2$ and $Q^2 \sim$ 1000-4000 GeV/$c^2$: For a given $Q^2$ scale, we find that the DO1 parametrization [14] gives the lowest cross section estimate while the highest is given by the GHR parametrization [15]. EHLQ I [16] gives an intermediate value. The band of uncertainty corresponding to these variations is ± 15%.

ii) the choice of the $Q^2$ scale: Various possibilities are $Q^2 \equiv \hat{s}$, $m_{top}^2 + p_T^2$, $m_{top}^2$, which correspond to variations of $Q^2$ by a little more than a factor 4 ( $\hat{s}$ is the square of the parton sub-process centre of mass energy ). $Q^2$ variations affect $\alpha_s(Q^2)$ as well as the parton densities. The lowest cross sections are obtained for $Q^2 = \hat{s}$ and the largest for $Q^2 = m_{top}^2$. The overall band of uncertainty corresponding to this variation of $Q^2$ is 34%. For example, for $m_{top} = 40$ GeV/$c^2$, the lowest cross-section value is obtained with DO1 and $Q^2 = \hat{s}$; $\sigma_O(t\bar{t}) = 0.45$ nb. The largest estimate comes from using GHR and $Q^2 = m_{top}^2$; $\sigma_O(t\bar{t}) = 0.9$ nb.

iii) The "K-factor" ( $\sigma(t\bar{t})/\sigma$[lowest order] ) associated with higher order Feynman graphs is not yet computed. Based on the K-factor for Drell-Yan processes in the same $Q^2$ range, we expect $K \leq 1.5$. In the absence of an exact calculation, we use the EUROJET Monte Carlo program [17] to obtain an estimate of the K-factor. In the EUROJET calculation, terms of order $\alpha_s^2$ and $\alpha_s^3$ are included using exact QCD matrix elements, but not including virtual gluon contributions. The calculation depends on an arbitrary cut-off on the $p_T$ of the soft gluon in the $O(\alpha_s^3)$ terms. This cut-off has been tuned on low $Q^2$ processes measured at the collider. Using the EHLQ I structure function with $\Lambda = 0.2$ GeV/$c^2$ and $Q^2 = m_{top}^2 + p_T^2$, EUROJET gives, for a top mass of 40 GeV/$c^2$, a cross section estimate $\sigma(t\bar{t}) = 1.1$ nb, corresponding to a K-factor of ~ 1.5.

In the following, we use the EUROJET cross section calculation as a reference value for our top rate predictions. At the end of the paper we discuss the effect of the uncertainty in $\sigma(t\bar{t})$ on our limit for the top mass. At the time of this analysis, EUROJET did not allow generation of complete events. We have therefore used the ISAJET Monte Carlo program, normalizing the cross section to the EUROJET estimate. The same fragmentation for the spectator jets is used that satisfactorily reproduces our data on $b\bar{b}$ and $c\bar{c}$ production [8]. ISAJET uses the exact $O(\alpha_s^2)$ QCD matrix elements for $t\bar{t}$ production and also includes gluon bremsstrahlung in the initial and final states. A heavy top quark is predicted to be produced centrally with a broad $p_T$ spectrum having $\langle p_T \rangle \sim m_{top}/2$.

### *3.3) Top fragmentation:*

As pointed out in our analysis of muon-jet events [8], the choices of fragmentation functions for charm and beauty strongly affect the inclusive muon rate. For top it is assumed that, because of its large mass, almost all the original top quark energy is transferred to the top hadron. For the fragmentation model, as in the case of charm and beauty, we use the parametrization of Peterson *et al.* [18] for the z-distribution of the top hadron :

$$D(z)dz = \frac{N}{z\left[1 - \frac{1}{z} - \frac{\varepsilon_t}{(1-z)}\right]^2} dz$$

- z is the fragmentation variable defined as $z = (E+p_L)_{hadron} / (E+p_L)_{quark}$.
- N is a normalization factor.

- $p_L$ is the longitudinal component of the momentum with respect to the quark axis.
- E is the energy evaluated in the same Lorentz frame as $p_L$, so that z is invariant with respect to Lorentz boosts along the quark axis.
- $\varepsilon_t = 0.5/ m_{top}^2$, which for a 40 GeV/$c^2$ top quark is approximately equal to $3x10^{-4}$. This results in a fragmentation function which is almost a $\delta$-function at $z = 1$ and is insensitive to the precise value of $\varepsilon_t$.

*3.4) Top decay modes:*

We assume that the $Q^2$ of the decays is sufficiently large that the decay of top hadrons can be computed at the quark level and that the final decay products are determined by the fragmentation algorithm. Once a top hadron is formed, the constituent top quark is decayed into a lepton, a neutrino and a b-quark jet (semi-leptonic decay) or into three quark jets (hadronic decay). For each lepton channel, V-A matrix elements are used and a branching ratio of 11% is assumed. For hadronic decays (branching ratio 66%), three body phase space and standard jet fragmentation are used.

*3.5) Event rates for semi-leptonic top decays:*

Fig. 1 shows the predicted rate for the production of the top quark at the collider in terms of the number of muon and electron events, for an integrated luminosity of 700 $nb^{-1}$, in which at least one top quark decays semi-leptonically. No selection cuts have been applied. For a top quark mass of 40 GeV/$c^2$, about 300 such semi-leptonic decays are expected. The contribution from $Z^0$ decays never exceeds 20% of the contribution from $W^{\pm}$ decays and disappears for top quark masses greater than half the $Z^0$ mass (46.5 GeV/$c^2$). For top quark masses between about 40 and 80 GeV/$c^2$ the production via W decays is predicted to dominate.

*3.6) Underlying event model:*

The correct simulation of the underlying event ( i.e. the contributions of spectator partons and gluon bremsstrahlung to the background energy flow ) is important because the isolation of the charged lepton is to be used as a criterion for distinguishing top quark production from other processes. The spectator contribution has been adjusted in ISAJET to reproduce the observed level of activity in W production and in charm and beauty events [8]. It is assumed that the same simulation is appropriate for $t\bar{t}$ production. This assumption is supported by the fact that, in jet data, the level of the underlying energy flow does not vary significantly with $Q^2$ in the range that is relevant for top production [19].

*3.7) Production and decay of a fourth generation quark:*

We have used a model for the production and decay of a fourth generation quark (b') similar to that used for the top quark , making the following assumptions and approximations:

- its electric charge is -1/3,
- its mass is lower than the top quark mass, so that it will not decay into a top quark,
- it is not produced in W decays,
- $b' \rightarrow c$ predominates over $b' \rightarrow u$,

The b' decay was computed in analogy to the top quark decay, with again a semi-leptonic decay branching ratio of 11% to each lepton, and the production of b' pairs from Z decays was neglected. We assume that the cross section for $b\bar{b}'$ production is identical to that for $t\bar{t}$, for the same quark mass, as expected from QCD. Note that, due to V-A matrix elements, the muon is harder in the decay $b' \rightarrow \mu$ than in $t \rightarrow \mu$.

*3.8) Monte Carlo production:*

High statistics Monte Carlo samples were generated for both the top quark (masses 25, 30, 40, 45, 50, 55 and 60 GeV/$c^2$, with a number of events at each mass equivalent to an integrated luminosity of at least 10 $pb^{-1}$), and for the b' quark (masses 30, 40 and 50 GeV/$c^2$, with a number of events equivalent to 10, 20 and 30 $pb^{-1}$ respectively). All the events were processed with detector simulation followed by event reconstruction, and analysed in the same way as real events.

## 4.- THE MUON CHANNEL

*4.1) The muon sample:*

The muon sample used corresponds to 556 $nb^{-1}$ ( 256 $nb^{-1}$ for 1984 and 300 $nb^{-1}$ for 1985 ). Because of changes in the muon trigger and improvements to the detector, a separate analysis of the acceptance and background would have been needed for the 1983 muon data which have therefore not been included. All events with a muon of transverse momentum ($p_T^{\mu}$) with respect to the beam axis larger than 6 GeV/c and satisfying the muon selection criteria described in [8] have been reconstructed yielding about 20,000 events. Technical details of the reconstruction procedures are given elsewhere [20]. This large inclusive muon sample has also been used to study the production of charm and beauty [8], which dominates at low $p_T^{\mu}$ after background subtraction, and W production which dominates at high $p_T^{\mu}$.

*4.2) Background to the muon signature:*

The background sources to the prompt muon signature are described in detail in [11]. The only substantial contribution comes from the decay in flight of charged pions and kaons. The method of calculating this background is described in [8]. Identical methods and data sets are used for this analysis.

*4.3) Data selection and comparison with Monte Carlo predictions:*

Fig. 2 shows the muon $p_T$ spectrum for the initial event sample with $p_T^{\mu} > 6$ GeV/c after subtraction of decay background. The Monte Carlo prediction for $b\bar{b}$, $c\bar{c}$, $J/\psi$, $\Upsilon$, Drell-Yan and W/Z reproduces both the shape and the normalization of the distribution. The predicted top quark contribution, shown for masses between 25 and 50 GeV/$c^2$, is small everywhere.

Selective cuts have been applied to increase the sensitivity to a possible top signal. It is instructive to illustrate the way in which the expected signal to noise ratio changes as the cuts are tightened on the muon and jets, as follows:

a) $p_T^{\mu} > 10$ GeV/c, $E_T^{jet1} > 12$ GeV, $m_T^{\mu\nu} < 40$ GeV/$c^2$, no jet 2 requirement;

b) $p_T^{\mu} > 12$ GeV/c, $E_T^{jet1} > 15$ GeV, $m_T^{\mu\nu} < 40$ GeV/$c^2$, no jet 2 requirement;

c) $p_T^{\mu} > 12$ GeV/c, $E_T^{jet1} > 15$ GeV, $m_T^{\mu\nu} < 40$ GeV/$c^2$, $E_T^{jet2} > 7$ GeV.

As already discussed, the lepton isolation is a principal tool for distinguishing top quark events from others. Figures 3(a), (b) and (c) show the data and the Monte Carlo predictions for the isolation variable, I , for the three sets of cuts. Also shown are the expected contributions for a top quark of 30 GeV/$c^2$ mass. It can be seen that in each case the whole distribution is well reproduced without the need for a contribution from a new heavy quark. If we restrict the selection to the region $I < 2$, for a top quark mass of 30 GeV/$c^2$, the expected signal to noise ratio is 0.3, 0.8 and 1.8 for cuts a), b), and c) respectively, as shown in Table 1. In this and subsequent tables, when two errors are quoted, the first is statistical and the second systematic. We have used the third set of cuts c), together with $I < 2$, as our selection for the top quark . The cumulative effects of the cuts on the efficiency for detecting a top quark of mass 40 GeV/$c^2$ are given in Table 2. After these cuts we observe 10 events with two or more jets in the data sample. The detailed comparison between data and Monte Carlo predictions is given in Table 3(a), together with the results for 1-jet events. The errors given on the top predictions (Table 3(b)) are statistical only. The expected contributions in the $\mu + \geq 2$ jets channel from $b\bar{b}$, $c\bar{c}$, W,Z, Drell-Yan, $J/\Psi$ and $\Upsilon$ amount to $9.2 \pm 0.8 \pm 1.0$ events, with another $2.3 \pm 0.4 \pm 0.7$ events from $K/\pi$ decays. This accounts well for the observed 10 events, without the need for an additional contribution from a top quark.

*4.4) $W \rightarrow \mu\nu$ events as a test of the Monte Carlo and detector models:*

The Monte Carlo generator was adjusted to reproduce the observed W transverse momentum distribution in the electron channel. The $W \rightarrow \mu\nu$ sample ($p_T^{\mu} > 15$ GeV/c, $m_T^{\mu\nu} > 40$ GeV/$c^2$) provides us with an important consistency check of our procedures. In Table 4, we compare the number of events found in the data for the various jet multiplicities to the numbers predicted by the Monte Carlo, which was tuned using the electron data. The excellent agreement shows that we understand the W simulation and selection procedures.

*4.5) Top cross section limits from muons:*

*4.5.a) Event rates --*

With the set of cuts c) we observe 10 isolated events with $I < 2$ and predict $11.4 \pm 0.9 \pm 1.2$ from non-top processes (table 3 (a)). Using Poisson statistics the data are consistent with at most 7.0 top events at 95% confidence level. In Fig. 4, this limit is compared to the predicted numbers of top quark events as a function of the top quark mass, where the shaded band is given by the experimental systematic errors. Shown also are the expected numbers of $W \rightarrow t\bar{b}$ events. By comparing the limit, which is based on event rate alone, to the predicted numbers, we obtain a lower limit on the top quark mass of 41 GeV/$c^2$ (95% c.l.). In extracting this limit we use the lower edge of the total systematic error band ( $\pm 1\ \sigma_{syst}$ ). The total systematic error, $\sigma_{syst}$, was computed by combining in quadrature an 8% error on the hadronic energy scale, 15% on the integrated luminosity for the prediction of the $t\bar{t}$ contribution, 10% on the simulation of the selection, 30% normalization error on the decay background and 50% on the Drell-Yan, J/$\psi$, and $\Upsilon$ backgrounds (see Table 3). The errors are discussed in more detail later, as are the effects of the uncertainties in the QCD prediction for the $t\bar{t}$ cross section.

*4.5.b) Kinematic distributions --*

An alternative way of deriving limits on the top cross section as a function of mass is to use the shapes of distributions of event properties that are able to differentiate between top and background processes. Taking events with at least two jets, and one muon with $p_T^{\mu} > 12$ GeV/c, we fit background and top contributions for a given top mass simultaneously to the distributions of the following four variables: the muon isolation variable I, $E_T^{\nu}$, $E_T^{jet1}$, and $|\cos \theta^*_{jet2}|$, where $\theta^*_{jet2}$ is the angle between jet 2 and the beam direction in the rest system of the muon, jet 1, jet 2 and the missing transverse energy. Gluon jets coming from initial state bremsstrahlung in $b\bar{b}g$ events tend to have large values of $|\cos \theta^*_{jet2}|$.

The background properties are taken from fully simulated $b\bar{b}$, $c\bar{c}$, W, Z, Drell-Yan, J/$\psi$, and $\Upsilon$ events. The limited statistics of the low $E_T$ jet sample used to calculate the background from

$\pi$ and K decays [8] do not allow us to use the shapes of the decay background distributions in each of the four variables in deriving the top cross section limits. However, from studying enlarged event samples, we find that the decay-in-flight muon is more isolated than in the $b\bar{b}$ and $c\bar{c}$ events while the shapes of the other three distributions are similar. The decay background is therefore not considered in fitting the data which is conservative since its inclusion would leave even less room for top.

Fits are made for various hypotheses about the top mass and the $t\bar{t}$ cross section, the $W \rightarrow t\bar{b}$ component being fixed. The resulting best fit value for the number of top events in the data, $n_{top}^{data}$, is in all cases very small (< 0.5 events). In order to find the confidence level to exclude a particular hypothesis we generate a large number of Monte Carlo experiments, each with the same integrated luminosity as the data. The fit is repeated for each experiment yielding different values for $n_{top}^{Monte\ Carlo}$. The number $n_{top}^{data}$ is then compared to the resulting distribution for $n_{top}^{Monte\ Carlo}$. We define the confidence level for excluding a particular cross section as the fraction of the Monte Carlo experiments with $n_{top}^{Monte\ Carlo} > n_{top}^{data}$.

The distributions for the four variables are shown in Fig. 5 for non-top processes, top with a mass of 40 GeV/$c^2$, and the data. The top selection cuts (10 events) were selectively loosened for certain distributions in order to provide a better normalization of the background in regions that are insensitive to top. Hence events are also considered in the fit if the muon is not completely isolated but passes all the other cuts, extending the range of the I-distribution from 2 to 10 (Fig 5a,104 events). In the same way the range of the $E_T^{jet1}$ distribution is extended down to 12 GeV with all other cuts applied (Fig 5c,17 events).

*4.5.c) Inclusion of Systematic Errors --*

Systematic errors are included by generating the distribution of $n_{top}^{Monte\ Carlo}$ with each uncertain parameter in turn fluctuated by its systematic error. Each error leads to a change in the confidence level. We derive the effect of all the errors by adding their individual effects in quadrature and subtracting this change in confidence level from the value obtained using only statistical errors.

The following systematic errors are included:

*Energy Scale:* The energy calibration combined with the simulation of the calorimeter response have an uncertainty of 8%. This affects the jet energies, the neutrino energy and the isolation of the muon. All these energy variations are assumed to be fully correlated.

*Selection Efficiency:* Since various small detector details are not simulated by the Monte Carlo, the predicted event rates may have errors arising from the detector response. An overall error of 10% from this source has been estimated.

*Integrated Luminosity:* An integrated luminosity error of 15% has been applied to processes not normalized by UA1 cross section measurements.

*$W \rightarrow t\bar{b}$ cross section:* Apart from the statistical error in the W cross section measurement (7%),

the $W \rightarrow t\bar{b}$ decay rate has higher-order QCD corrections of 10-20%, which have an error of 30%. Combination of these two errors gives uncertainties between 10% (light top) and 14% (heavy top).
*Dimuons:* The rate of high $p_T$ dimuon events in which only one of the muons is detected has been estimated from our own data. The contributions from large $p_T$ Drell-Yan, J/$\psi$, and $\Upsilon$ have a normalization error of 50%.
*Fragmentation:* The $\varepsilon$ parameter of the b quark Peterson fragmentation function [18] has been varied between 0.001 and 0.1 with no appreciable effect on the shapes of the distributions used in the fit. This variation covers the range of accepted values from $e^+e^-$ experiments.

*4.5.d) Conclusion --*

The results for the 90% and 95% confidence level upper limits on the cross section are shown as a function of top quark mass in Fig. 6 together with the predicted cross section. The conclusion from this analysis of the muon data is that a top quark of mass smaller than 43 GeV/$c^2$ is excluded with 95% confidence if the predicted cross section is correct. The effect of uncertainties in the QCD calculation will be discussed later.

## 5.- THE ELECTRON CHANNEL

### *5.1) The electron sample:*

During the 1983, 1984 and 1985 runs the electron trigger selected events satisfying the requirement that in two adjacent cells of the electromagnetic calorimeters the measured transverse energy ($E_T$) was larger than 10 GeV. A simple on-line selection using 168E processors, requiring a rough isolation of the electromagnetic cluster, reduced the data to about $10^6$ events. Finally, all events with a reconstructed cluster $E_T$ (after calibration) larger than 10 GeV and having a central detector track matching the cluster were fully reconstructed. For the heavy quark search we have used the sample of events with $E_T > 15$ GeV, where the background is lower. The total integrated luminosity for this sample is 689 $nb^{-1}$.

### *5.2) Electron identification:*

An electron is identified by the presence of a high $p_T$ ($p_T > 10$ GeV/c) charged track associated with an electromagnetic cluster ($E_T > 15$ GeV) and satisfying the following selection criteria:

- matching within 3 standard deviations in momentum and position between the cluster and the track.

- cut on the shape of the shower profile in depth. An energetic electron deposits almost all of its energy in the four segments of the electromagnetic calorimeter ( 27 radiation lengths at normal

incidence ) and only a small fraction in the two hadronic compartments behind. A cut on the hadron calorimeter energy in the cells behind the electromagnetic cluster is applied, $E_{had} < 200$ MeV. In addition a $\chi^2$ cut is applied on the compatibility of the deposition in the four electromagnetic segments with an electromagnetic shower profile.

- electron isolation. As will be discussed in the following section, the dominant background for the electron signature comes from jet fluctuations, either converted photons from $\pi^0$ decays or low multiplicity jets where a high $p_T$ charged pion overlaps with photons from $\pi^0$ decays. Strict isolation requirements around the electron direction together with electromagnetic shower profile requirements are used to minimize this background. The sums $\Sigma p_T$ (additional tracks) and $\Sigma E_T$(calorimeter cells) in a cone $\Delta R \equiv (\Delta\eta^2+\Delta\phi^2)^{1/2} = 0.7$ around the electron are each required to be less than 10% of the electron transverse energy, and less than 1 GeV in a cone $\Delta R = 0.4$.

After these cuts, 291 events remain. The isolation requirement also rejects electrons coming from beauty and charm decays, because they are usually embedded in jets, and therefore already enhances the top signal; the loss of efficiency for genuinely isolated electrons has been estimated to be about 20% using electrons coming from W decays.

*5.3) Photon conversions:*

This sample is still contaminated by electrons coming from photon conversion. Events were scanned, using a Megatek graphics display, to remove remaining conversions in the following cases :

- the second electron from the pair is observed in the central detector and the pair kinematics are compatible with a converted photon,
- the conversion occurs far from the interaction vertex, so that the track begins in the middle of a central detector module, with or without a visible partner, and can easily be identified,
- the specific energy loss (dE/dx) measurement identifies the event as one in which the $e^+$ and the $e^-$ are not separated by the magnetic field .

After scanning, the sample is reduced to 205 events, 75 events having been identified as conversions and the remaining 11 discarded because of reconstruction problems or because of the presence of a second interaction. The estimation of the non identified conversions will be discussed in section 5.5.

*5.4) Data Classification:*

The 205 electron events with $E_T^e > 15$ GeV are divided into three categories: 119 events have $m_T^{ev} > 45$ GeV/$c^2$ and are classified as W candidates. 26 events have a second electron candidate, defined by a charged track in the central detector with $p_T > 5$ GeV/c pointing to an

isolated electromagnetic cluster with $E_T > 6$ GeV in the calorimeter, and are classified as dielectron events. These events are background free and are well understood in terms of W, Z, Drell-Yan, J/Ψ and Υ production. Table 5 shows a comparison between the data and the Monte Carlo predictions for these processes according to the number of jets. As can be seen, there is excellent agreement. Finally, the remaining 60 events are classified according to their topology: 34 events have no jet, 19 have one jet and 7 are produced with two jets, where the jets are defined as described in *2.3.a)*. We now discuss the background from fake electrons to these 60 events.

*5.5) Electron background calculations:*

As discussed above, the two main background sources are $\pi^{\pm}\pi^0$ overlaps and remaining converted photons, mainly from $\pi^0$s. We explain here the techniques used to calculate these backgrounds; more details can be found elsewhere [21].

The main background comes from jets faking an electron signal by fragmenting into an energetic charged pion accompanied by one or more photons in the same calorimeter cell, the whole system satisfying the electromagnetic shower profile requirements. The absolute yield of isolated $\pi^{\pm}\pi^0$ events is estimated from a data sample of charged pions which may be accompanied by $\pi^0$s. These "isolated pions" are selected from the electron trigger sample ( $E_T > 10$GeV), requiring track quality, matching and isolation criteria identical to those used for the electron selection. However, the shower profile requirement in the electromagnetic calorimeter is changed to an energy deposition requirement ($E_{had} > 1$GeV) in the associated hadron calorimeter cells. To get the absolute yield of isolated $\pi^{\pm}\pi^0$ events, each of the selected $\pi^{\pm}(+n\ \pi^0)$ is weighted by the inverse of the probability to have fulfilled the electron trigger conditions and passed the hadronic energy cut. This probability is obtained from pion beam data with superimposed simulated $\pi^0$s; probabilities are tabulated as a function of charged energy, $\pi^0$ content and angle of incidence. These overlapping $\pi^{\pm}(+n\pi^0)$ Monte Carlo 'tracks' are then used to calculate the probability that each selected "isolated pion" would have fulfilled the shower profile criterion to become a background candidate to electron - jet events. Table 6 shows the result of this calculation for various jet multiplicities. The first error quoted is statistical and comes only from the limited sample of isolated pions (523 events) selected from the data. The second error is systematic and comes from two sources: the limited statistics of the test beam data and the unknown electron contamination of the pions in the beam. This overlap background alone is not sufficient to explain the observed rate of electron events.

To test the $\pi^{\pm}(+n\pi^0)$ overlap background calculation, the predicted rate of overlap events is estimated, for the events with at least one jet, as a function of $E_{had}$, the hadronic energy deposition in the cells behind the electromagnetic cluster. The predicted rate of overlaps is compared to the data as function of $E_{had}$ in Fig. 7. The bin $0 < E_{had} < 0.2$ GeV contains the 26 isolated electron

candidates accompanied by at least one jet (19 one-jet and 7 two-jet events). The overlap background estimate with this calculation is $6.3 \pm 0.5 \pm 1.1$ events in this bin as already shown in Table 6. For large values of $E_{had}$ the overlap background is expected to dominate the data and we can therefore check the overlap background estimate. For $E_{had} > 0.5$ GeV there is good agreement between predicted and measured background.

The next most important source of background comes from the conversion of $\pi^0$ decay photons. As described above, a large fraction of these conversions are removed by scanning; however, a converted photon may be missed in one of the following cases :

- the conversion occurs close to the interaction vertex and one of the converted electrons does not emerge from the beam tube,
- the electron belongs to a Dalitz pair, and the second electron cannot be identified.

Two methods have been used to calculate this background. The first is an analytic calculation, using a data sample of high $p_T$ $\pi^0$s satisfying the isolation and electromagnetic shape requirements used for electron identification. Taking into account the known amount of material in the detector, we then calculate the probability of an asymmetric conversion in which one member of the electron pair has $p_T < 50$ MeV/c and is not reconstructed in the detector. In the second method, $\pi^0$s and single photons are generated by Monte Carlo techniques and their conversions fully simulated. The events in which one of the electrons satisfies the electron selection criteria are then scanned and the fraction of conversions identified is measured. By comparing this result with the number of identified conversions in the data we obtain an estimate of the background of unidentified conversions.

The methods are in good agreement and the results are presented in Table 6 according to the number of jets observed in the event. For the 26 electron + $\geq$ 1 jet events, the conversion background is $1.8 \pm 0.7$ events.

*5.6) Comparison with Monte Carlo predictions:*

We now estimate the contributions from known sources of real electrons to the 60 single electron events with $m_T^{ev} < 45$ GeV/$c^2$, including electron pair events in which only one electron is detected, and compare them with the data. The strict isolation criteria that are necessary to select electrons are already tighter than those used in the top search in the muon channel. The efficiency for detecting a top quark of mass 40 GeV/$c^2$ in events with at least one jet is given in Table 7. As described above, a large Monte Carlo production for all electron sources has been performed including the following processes: $W \rightarrow e\nu, \tau\nu$, $Z \rightarrow e^+e^-$, Drell-Yan, $J/\psi$ and $\Upsilon$, $b\bar{b}$ or $c\bar{c}$ producing high $p_T$ electrons. We make full use of our present knowledge about the transverse momentum distributions of the Ws and Zs [22], as well as of muon pairs from Drell-Yan, $J/\psi$ and $\Upsilon$ [11]. Table 8 summarizes all electron contributions and corresponding backgrounds, according to event topology. The first error quoted in each entry is the statistical error from the

Monte Carlo; the second is the systematic error, which is discussed below.

For the W, Z, Drell-Yan, J/$\psi$, and $\Upsilon$ the expected rates in the high $p_T$ tails are normalized to our data. For the latter three processes, which are measured in the dimuon channel, we assign a systematic error of $\pm$ 50% to the rates in these tails. In addition, our determination of the cross sections for Drell-Yan, J/$\psi$, and $\Upsilon$ production are only accurate to 30% (again using measured dimuon events [11]).

The contributions from $b\bar{b}$ and $c\bar{c}$ are normalized to our measurements of these processes using muon-jet events [8]. According to Monte Carlo studies, an electron from charm is three times as likely to be selected as one from beauty because of the large cell size of the central calorimeter, and we assign a 25% systematic error to this part of the top electron background, which arises from the uncertainty on the relative contributions of $b\bar{b}$ and $c\bar{c}$ to the muon-jet sample [8].

With the electron sources discussed here and summarized in Table 8, the observed event rate is explained for all topologies, without the need for a new heavy quark contribution. As shown in Table 8(b), the Monte Carlo rate for the electron background agrees with the data even when the sample of electron-jet events is enlarged by lowering the $E_T$ cut to 12 GeV. Arranging events by jet multiplicity also shows agreement in rate between the Monte Carlo prediction and the data, even though different processes may dominate for different multiplicities.

As in the muon case, the non-top background processes account well for the detailed features of the electron events. In Fig. 8 we display the distributions of four variables characteristic of the properties of the 26 events with at least one jet, together with the expected shapes for the non-top background: $E_T^e$, $E_T^{jet1}$, $\Delta\phi$(e,jet1), $\cos\theta^*_{jet2}$. The agreement is good. Unlike in the case of muons, the isolation properties of electrons cannot be studied easily because one can only define a low background sample for isolated electrons. However, tests made with less restrictive isolation requirements do not change the conclusions: that the rate and properties of events with an electron and various numbers of jets is well accounted for by known sources.

The expected rates from top quark sources are summarized in Table 9 as a function of mass.

### *5.7) Top cross section limits from electrons:*

#### *5.7.a) Event rates --*

The data are consistent with at most 12 events (95% c.l.) with $\geq$ 1 jet , $p_T^e > 15$ GeV/c and $m_T^{ev} < 45$ GeV/$c^2$, coming from the production of a top quark. Fig. 9 shows the comparison between this limit and the predicted number of top quark events as a function of the top quark mass. The shaded band is given by the total systematic errors. Shown also are the expected numbers of $W \rightarrow t\bar{b}$ events. Comparing the limit to the predicted numbers, we obtain a lower limit on the top quark mass: $m_{top} > 36$ GeV/$c^2$ (95% c.l.). In extracting this mass, we use the lower edge of the systematic error band. The individual systematic errors are added in quadrature as in the

muon case.

*5.7.b) Kinematic distributions --*

An analysis of the shapes of kinematic variable distributions leads to a stronger limit on the top contribution to the data sample. A study of kinematic variables, $E_T^e$, $E_T^\nu$, $m_T^{e\nu}$, $E_T^{jet1}$, $\Delta\phi_{e\nu}$, $\cos\theta^*_{jet2}$, has enabled their separating power to be quantified. The following two distributions are found to be the most powerful in the electron channel:

- the neutrino transverse energy spectrum displayed in Fig. 10(a) for "background events", defined as the list of contributions given in Table 8(a), for W's and for top-decay electrons from a top quark of 40 GeV/$c^2$ mass: Top quarks are expected to give events with neutrino transverse energies in a region where the contribution from W's as well as from the background processes are expected to be small. The curves are normalized to the expected event rate of each contribution, for a total integrated luminosity of 689 $nb^{-1}$,

- the number of jets in the event: Top quarks contribute more to events with $\geq 2$ jets; this effect is more striking for increasing top mass, but the expected rates are lower. The experimental measurements together with the expected rates for top and background processes are shown in Fig. 10(b).

We use the method described above for the muon case to extract the limits on the top cross section for a given mass, normalizing the $W \rightarrow e\nu$ contribution to the cross-section measured by UA1 and treating the systematic errors in the same way as for muons.

*5.6.b) Systematic errors --*

The systematic errors include:

*Background rate:* The overall uncertainty on the rate of background events (overlaps, conversions, W/Z, $b\bar{b}$, $c\bar{c}$, Drell-Yan, J/$\Psi$,$\Upsilon$ ) is ~ 12%.

*Energy scale:* The uncertainties in the energy scale are 3% for electrons, 5% for neutrinos, and 8% for jets. All these uncertainties are correlated.

*Selection efficiency:* As in the muon case, this is estimated to be 10%.

*$W \rightarrow t\bar{b}$ cross section:* The error on the estimate of the $W \rightarrow t\bar{b}$ cross-section, including the lack of knowledge of the QCD corrections, is 10% (light top) to 14% (heavy top).

*Integrated luminosity:* The error on the integrated luminosity, 15%, applies to the $t\bar{t}$ events only, because the W cross section is measured in the experiment.

*5.7.d) Conclusion --*

The 90% and 95% confidence level cross section limits are shown in Fig. 11, together with the predictions, as a function of the top quark mass. A top mass below 47 GeV/$c^2$ is excluded with 95% confidence if the predicted cross section is correct. The effect of uncertainties in the QCD calculation will be discussed later.

## 6.- COMBINED LIMIT FROM MUONS AND ELECTRONS

*6.1) Global fit:*

Using the four muon variables ( I, $E_T^{\nu}$, $E_T^{jet1}$, $|\cos\theta^*_{jet2}|$) and the two electron variables ($E_T^{\nu}$, $N^{jets}$), in a global fit, gives a better limit on the top quark cross section, which is shown as a function of mass in Fig. 12. It can be seen that the experiment is not sensitive to the process $W \rightarrow t\bar{b}$ alone. A limit on the top quark mass can only be obtained if the contribution from $p\bar{p} \rightarrow t\bar{t}\,X$ is taken into account. Using the full cross section prediction described in Section *3.2b*, a top quark mass lower than 56 GeV/$c^2$ is excluded at 95% confidence level.

*6.2) Effect of QCD uncertainties:*

In order to explore the sensitivity of this mass limit to details of the QCD calculation, in Fig. 13 we show our 95% confidence level cross section limit, with the $W \rightarrow t\bar{b}$ cross section subtracted, expressed in terms of the calculated $t\bar{t}$ cross section, $\sigma(t\bar{t})$. We display our limit in terms of the variable $K = \sigma(t\bar{t}) / \sigma_0$, where $\sigma_0$ is the lowest order QCD cross section calculated with the EHLQ I structure functions and $Q^2 = m_{top}^2 + p_T^2$. Shown in the figure is a range of predictions to lowest order as well as the EUROJET calculation ($K \simeq 1.5$) from which the above limit (> 56 GeV/$c^2$) was derived. If instead, we use the structure functions (DO1) and definition of $Q^2$ ( $= \hat{s}$) that give the lowest value of the cross section, we obtain a lower limit of 44 GeV/$c^2$ at 95% confidence level (see Fig. 13).

## 7.- CROSS SECTION LIMITS FOR b'

For the b'-quark, we employ the same method used for the top quark except that, in this case, there is assumed to be no contribution from W decays. Fig. 14 shows the 95% confidence level limits on the b' cross section as a function of the b' mass, using the combined electron and muon information. For the EUROJET QCD cross section, a mass below 44 GeV/$c^2$ is excluded at 95% confidence level. The lowest order calculation that was used for $t\bar{t}$ gives $m_{b'} > 32$ GeV/$c^2$ (95% c.l.)

## 8.- LIMITS FROM MUON PAIRS

Events containing one or two top quark decays will have a significant probability to contain a lepton pair. The number of lepton pairs coming from top is expected to be smaller that the number of lepton - jet events but the results should give consistent limits on the production of new heavy quarks.

The most sensitive channel in our case is muon pairs.The dimuon sample described in [11]

is used. Each muon has a $p_T$ larger than 3 GeV/c and the muon pair mass, $m_{\mu\mu}$, is larger than 6 GeV/$c^2$. The number of such muon pairs expected from top quark production is given in Table 10 as a function of the top quark mass.

To distinguish between dimuons from top quark decays and those from charm and beauty decays we make use of the different event kinematics resulting from the much larger mass of the top quark. The following event properties are used:

- $p_T^{\mu 1}$, $p_T^{\mu 2}$, where $\mu 1$ and $\mu 2$ are the highest $p_T$ and next to highest $p_T$ muons,
- $\Delta\phi$, the azimuthal angle difference between the two muon directions,
- $E_T^{\nu}$, the missing transverse energy,
- $N^{jet}$ the number of jets with $|\cos(\theta^*)| < 0.8$.

Using the shapes of the distributions for these five variables, $X_i (i=1,5)$, for top and non-top processes, we define a "top likelihood" for each event as:

$$\mathfrak{L}(m_{top}) = \Pi_i \, [p_{top}(X_i)/p_{beauty}(X_i)],$$

where $p_{top}(X_i)$ and $p_{beauty}(X_i)$ are the probability density functions of the variables $X_i$ for a top quark of mass $m_{top}$ and for $b\bar{b}$ and $c\bar{c}$ events passing the dimuon cuts, and $\Pi$ indicates a product over the index i (i = 1,5) of the five distributions. Fig. 15 shows the comparison between the $\ln(\mathfrak{L}(m_{top}=25\ \text{GeV}/c^2))$ distributions for i) non-top processes, ii) $t\bar{t}$ events with a 25 GeV/$c^2$ top mass and iii) the data.

The muon pair sample described in [11] is enriched in potential top candidates by requiring a mild isolation of the muons ( $\Sigma E_T < 9$ GeV for each muon, where $\Sigma E_T$ is the sum of the calorimeter transverse energy in a cone $\Delta R < 0.7$ ). Comparing our data with Monte Carlo predictions for $b\bar{b}$, $c\bar{c}$, Drell-Yan and decay background in the region where $\ln(\mathfrak{L}(\, m_{top}\,))$ is larger than 2, we obtain limits on the production of a top quark as a function of its mass, as shown in Fig. 16.

Assuming the EUROJET QCD prediction for $t\bar{t}$, we obtain $m_{top} > 33$ GeV/$c^2$ (95% c.l.). This limit can also be interpreted as a limit on the b' mass ($m_{b'} > 33$ GeV/$c^2$) since it does not involve the $W \rightarrow t\bar{b}$ process, which was not included because its contribution to dimuons is relatively small in the low mass range where we are sensitive. The conservative lowest order cross section calculation, described in section 6.2, gives a top mass limit of 23 GeV/$c^2$ at 95% confidence. These limits are, as expected, weaker than the ones obtained in the electron -jet and muon - jet channels but are consistent. Furthermore, they help to exclude low masses.

The electron pair ( 21 events with $m(e^+e^-) < 60$ GeV/$c^2$ ) and electron-muon pair ( 8 events with $p_T^{\mu} > 3$ GeV/c ) channels have also been studied. In both cases, because of the higher threshold ( $E_T^e > 8$ GeV) imposed at the trigger level, the sensitivity to a new heavy quark is lower than in the case of muon pairs, and does not give us extra information on the top quark mass. In both cases the number of events found in the data agrees with our prediction for standard sources.

## 9.- DISCUSSION OF RESULTS

We have described a search for new heavy quarks using isolated muons or electrons associated with jets. A detailed analysis shows that background contributions from known sources are able to account for the observed data without the need for a new quark. Taking into account both statistical and systematic errors we have extracted upper limits on the production cross-sections for top and b' quarks consistent with the data, assuming a semi-leptonic branching ratio of 11%.

### *9.1) The $W \rightarrow t\bar{b}$ process:*

Our basic result is a limit on the cross section for producing new heavy quarks (t or b') as a function of the quark mass. Although the expected $W \rightarrow t\bar{b}$ cross section can be estimated quite reliably from our own $W \rightarrow l\nu$ data, with the present detector and integrated luminosity (~ 700 $nb^{-1}$), the experiment is insensitive to this process for all masses. To become sensitive, a factor 4 increase in integrated luminosity or an equivalent improvement in efficiency would be needed and can be expected for the upgraded detector using the improved collider with ACOL [23].

### *9.2) QCD production of $t\bar{t}$ pairs:*

A limit on the top quark mass can only be obtained by including the more uncertain $t\bar{t}$ process in the estimation of the expected rate, which has to be calculated using QCD. The most conservative approach is to take only the lowest order terms and to use the structure functions (DO1 [14]) and $Q^2$ scale ($Q^2 = \hat{s}$) that give the smallest cross section. Using the combined muon-jet and electron-jet data we find:

$$m_{top} > 44 \text{ GeV}/c^2 ; \quad m_{b'} > 32 \text{ GeV}/c^2$$

at 95% confidence level. Using the EUROJET estimate of the order $\alpha_s^3$ terms in the calculation of the $t\bar{t}$ cross section and taking less pessimistic choices for the structure functions (EHLQ I [16]) and $Q^2$ scale ($Q^2 = m_{top}^2 + p_T^2$), the limits become $m_{top} > 56$ GeV/$c^2$ and $m_{b'} > 44$ GeV/$c^2$, both at 95% confidence level.

At low masses, our limits overlap with the PETRA and TRISTAN lower limits, leaving no lower mass window. In fact, due to the additional information provided by the muon pair channel, our sensitivity at low top quark masses is even better than indicated in Fig. 12 where only single lepton data have been used.

From muon pairs alone, the lower limit on the top quark mass corresponding to the EUROJET QCD calculation is 33 GeV/$c^2$ (95% c.l.). This is also a lower limit on the mass of the b' quark, since in the muon pair analysis the process $W \rightarrow t\bar{b}$ was not included and the muon is

harder in the decay $b' \rightarrow \mu$ than in $t \rightarrow \mu$.

*9.3) Sensitivity to a top quark above the W mass:*

If the top quark is heavier than the W, an interesting situation occurs. The top quark can decay into a real W, so that the process $p\bar{p} \rightarrow t\bar{t}X$ leads to a final state with two real large $p_T$ Ws. The average $p_T$ of each top quark with respect to the beam axis is $\langle p_T(top) \rangle \sim m_{top}/2$. In the decay $t \rightarrow Wb$, the W, because of its mass, will carry most of the transverse momentum of the parent top and is therefore also produced at large $p_T$: $\langle p_T(W) \rangle \sim 45$ GeV/c. If one of the Ws decays into $e\nu$ ( or $\mu\nu$ ) and the other into two jets, the resulting $l\nu jj$ topology is similar to the QCD production of a large $p_T$ W balanced by two jets. UA1 has observed two Wjj events with $p_T(W) > 80$ GeV/c and $m(jj) \sim m(W)$ [22]. In the kinematic range where the events are observed, $0.05 \pm 0.03$ events are predicted for QCD W production and $0.02^{+0.02}_{-0.01}$ events for $t\bar{t}$ production with $m_{top} = 90$ GeV/$c^2$. No conclusion can be drawn with the present statistics.

The improved UA1 detector at ACOL should clarify the situation. The dash-dotted curve in Fig. 1 shows the expected yield of W pairs as a function of $m_{top}$, when one W decays into $e\nu$ or $\mu\nu$ and the other into two jets with $m_{jj} > 70$ GeV/$c^2$. About 10–20 events are expected for $m_W < m_{top} < 100$ GeV/$c^2$ for $\int Ldt = 700$ nb$^{-1}$.

*9.4) Compatibilty with results from the 1983 collider run:*

In our earlier results [7], based on 1983 data alone, there were 3 electron events and 4 muon events satisfying similar criteria to those that have been used to select the data with $\geq 2$ jets. With the present cuts, 7 and 10 events, respectively, are observed in the full data samples. Given the ratios of the integrated luminosities between the present and earlier data samples, we would have expected 1.1 electron and 1.9 muon events in the 1983 data sample. At that time, our background estimates did not include the $J/\psi$, $\Upsilon$ and Drell-Yan contributions. Also, our estimate of the $b\bar{b}$ and $c\bar{c}$ background for isolated muons is now four times higher because of a better understanding of the $b\bar{b}$ and $c\bar{c}$ rates and properties. Finally our muon decay background estimate has been improved by using higher statistics low energy jet data samples. Although the 1983 events have the expected top quark topology, we conclude that they are most likely due to background sources.

*9.5) Mass distributions:*

In the foregoing analysis we have not made use of invariant mass distributions in searching for a new quark signal. In Figs. 17 and 18, we plot the invariant masses of the lepton–transverse neutrino–jet 1–jet 2 (M4) and lepton–transverse neutrino–jet 2 (M3) systems for the muon and

electron data respectively. The data are well simulated by the Monte Carlo without top, but the prediction for top (for a mass of 40 GeV/$c^2$) does not have a significantly different shape. The shape of the mass distribution for the background is constrained by the procedure devised to select top events and cannot be used to provide useful additional discrimination.

*9.6) Conclusion:*

The results of this search, in which no evidence has been found for a new heavy quark, have provided a lower limit on the top quark mass ( > 44 GeV/$c^2$), with rather conservative assumptions about the production cross section. The limit is in an interesting region as it implies that the $Z^0$ may not be able to decay into $t\bar{t}$. If this is so, W decays offer the best way of finding the top quark for masses up to ~ 75 GeV/$c^2$. For masses above the W mass, the top quark will decay into a W giving typically events with two high $p_T$ Ws where one W decays semi-leptonically and the other decays into a pair of jets.

## Acknowledgments

We are thankful to the management and staff of CERN and of all participating institutes for their vigorous support of the experiment. The following funding agencies have contributed to this programme:

Fonds zur Förderung der Wissenschaftlichen Forschung, Austria.
Valtion luonnontieteellinen toimikunta, Suomen Akatemia, Finland.
Institut National de Physique Nucléaire et de Physique des Particules and
Institut de Recherche Fondamentale (CEA), France.
Bundesministerium für Forschung und Technologie, Fed. Rep. Germany.
Istituto Nazionale di Fisica Nucleare, Italy.
Science and Engineering Research Council, United Kingdom.
Stichting Voor Fundamenteel Onderzoek der Materie, The Netherlands.
Department of Energy, USA.
The Natural Sciences and Engineering Research Council of Canada.

Thanks are also due to the following people who have worked with the collaboration in the preparations for and data collection on the runs described here: L.Baumard, F.Bernasconi, D. Brozzi, R.Conte, L.Dumps, G.Fetchenhauer, G.Gallay, J.C. Michelon and L.Pollet.

**Table 1:** TOP and Non-TOP contributions for isolated ( I < 2 ) muon events with three different sets of cuts. The first error is statistical, the second one systematic.

| | | MONTE CARLO | | |
|---|---|---|---|---|
| | Data | non - TOP | TOP ($m = 30$ GeV/$c^2$) | TOP/non-TOP |
| Cut Set a) | 140 | $143 \pm 7 \pm 22$ | $44 \pm 7$ (syst) | 0.3 |
| Cut Set b) | 32 | $35 \pm 2 \pm 5$ | $29 \pm 4$ (syst) | 0.8 |
| Cut Set c) | 10 | $11.4 \pm 0.9 \pm 1.2$ | $20.5 \pm 3$ (syst) | 1.8 |

**Table 2:** Efficiency for detecting TOP quark events in the muon channel.The number of events corresponds to 556 $nb^{-1}$ for a TOP mass of 40 GeV/$c^2$.

| | $t\bar{b}$ | $t\bar{t}$ |
|---|---|---|
| All events with a muon | 89 (100%) | 129. (100%) |
| $P_T^{\mu} > 12$ GeV/c | 37.5 (42.2%). | 55.8 (43.3%) |
| reconstructed $P_T^{\mu} > 12$ GeV/c $E_T^{jet1} > 15$ GeV | 10.4 (11.7%) | 15.0 (11.6%) |
| $E_T^{jet2} > 7$ GeV | 5.8 (6.5%) | 12.1 (9.4%) |
| I < 2 | 4.0 (4.5%) | 7.0 (5.4%) |
| $m_T^{\mu\nu} < 40$ GeV/$c^2$ | 3.6 (4.0%) | 6.0 (4.6%) |

**Table 3(a): Sources of isolated Muon + Jet Events.**

**$P_T^{\mu} > 12$ GeV/c**

**The first error is statistical, the second one systematic.**

| | MONTE CARLO | | | | | DATA |
|---|---|---|---|---|---|---|
| | K /π Decays | W/Z | D.Y. J /Ψ ϒ | $b\bar{b}$ $c\bar{c}$ | TOTAL | |
| μ + 1 jet | 7.2 ± 1.7 ± 2.2 | 2.5 ± 0.5 | 7.3 ± 0.7 ± 3.6 | 6.3 ± 0.6 | **23.3 ± 2.0 ± 4.2** | **22** |
| μ + ≥2 jets | 2.3 ± 0.4 ± 0.7 | 0.6 ± 0.2 | 2.0 ± 0.4 ± 1.0 | 6.6 ± 0.7 | **11.4 ± 0.9 ± 1.2** | **10** |

**Table 3(b): Expected TOP Event Rates for Isolated Muons with $p_T^{\mu} > 12$ GeV/c .**

*Number of jets = 1 :*

| | TOP MASS ( GeV/$c^2$ ) | | | |
|---|---|---|---|---|
| | 25 | 30 | 40 | 50 |
| $t\bar{b}$ | 2.3 ± 0.3 | 3.3 ± 0.5 | 2.8 ± 0.4 | 1.7 ± 0.3 |
| $t\bar{t}$ | 7.1 ± 0.6 | 5.0 ± 0.5 | 1.4 ± 0.2 | 0.5 ± 0.1 |
| **Total** | 9.4 ± 0.7 | 8.3 ± 0.7 | 4.2 ± 0.4 | 2.2 ± 0.3 |

*Number of jets ≥ 2 :*

| | TOP MASS ( GeV/$c^2$ ) | | | |
|---|---|---|---|---|
| | 25 | 30 | 40 | 50 |
| $t\bar{b}$ | 2.5 ± 0.3 | 3.9 ± 0.6 | 3.6 ± 0.5 | 3.1 ± 0.5 |
| $t\bar{t}$ | 21.8± 1.1 | 16.6 ± 0.9 | 6.0 ± 0.5 | 2.2 ± 0.3 |
| **Total** | 24.3 ± 1.1 | 20.5 ± 1.1 | 9.6 ± 0.7 | 5.3 ± 0.6 |

All the errors quoted here are statistical only.

**Table 4: W Selection in the Muon Channel.**

$P_T^{\mu} > 15$ GeV/c, $m_T(\mu,\nu) > 40$ GeV/$c^2$

Isolation : $\Sigma E_T < 3$ GeV , $\Sigma P_T < 2$ GeV/c, $\Delta R < 0.7$

| | MONTE CARLO | DATA |
|---|---|---|
| $\mu$ + 0 jets | $64 \pm 2$ | 57 |
| $\mu$ + 1 jet | $9 \pm 1$ | 8 |
| $\mu$ + $\geq$ 2 jets | $1.5 \pm 0.5$ | 3 |

**Table 5: a) W Selection in the Electron Channel.**

$E_T^e > 15$ GeV, $m_T(e,\nu) > 45$ GeV/$c^2$

| | MONTE CARLO | | | | | DATA |
|---|---|---|---|---|---|---|
| | W | Z | D.Y. J/Ψ ϒ | $b\bar{b}$ $c\bar{c}$ | TOTAL | |
| e + 0 jets | 98 ± 2.3 | 0.7 ± 0.3 | 0.64 ± 0.37 | 0.1 ± 0.1 | **99.4 ± 2.3** | **101** |
| e + ≥ 1 jets | 15.4 ± 1.2 | 0.5 ± 0.2 | 0.1 ± 0.06 | 0.1 ± 0.1 | **16.1 ± 1.2** | **18** |

**b) electron pairs.**

$E_T(e_1) > 15$ GeV, $E_T(e_2) > 5$ GeV.

| | MONTE CARLO | | | | | DATA |
|---|---|---|---|---|---|---|
| | W | Z | D.Y. J/Ψ ϒ | $b\bar{b}$ $c\bar{c}$ | TOTAL | |
| Pair + 0 jets | 0.12 ± 0.08 | 15.9 ± 1.0 | 4.9 ± 1.7 | 0.1 ± 0.1 | **21.0 ± 2.7** | **21** |
| Pair + ≥1 jets | 0.56 ± 0.2 | 7.2 ± 0.6 | 1.35 ± 0.46 | 0.1 ± 0.1 | **9.2 ± 0.93** | **5** |

**Table 6:** **Backgrounds to the electron signature for the 60 events with : $E_T^e > 15$ GeV, $m_T(\nu, \mu) < 45$ GeV/$c^2$.**

| | Data | Overlaps | Conversions |
|---|---|---|---|
| e + 0 jets | 34 | $2 \pm 0.2 \pm 0.5$ | $1.0 \pm 0.5$ |
| e + 1 jet | 19 | $4 \pm .35 \pm 1.0$ | $1.5 \pm 0.7$ |
| e + ≥ 2 jets | 7 | $2.3 \pm 0.3 \pm 0.5$ | $0.3 \pm 0.1$ |

**Table 7:** **Efficiency for detecting TOP quark events in the electron channel.The number of events corresponds to 690 $nb^{-1}$ for a TOP quark mass of 40 GeV/$c^2$.**

| | $t\bar{b}$ | $t\bar{t}$ |
|---|---|---|
| All events with an electron | 110. (100%) | 160. (100%) |
| $E_T^e > 15$ GeV | 29. (26%) | 44. (27%) |
| CD track $P_T > 10$ GeV/c | 23.5 (21%) | 35.5 (22%) |
| Isolation | 10. (9%) | 10.5 (6.5%) |
| Electromagnetic shower shape | 6.2 (5.6%) | 7.2 (4.5%) |

**Table 8:** Classification of Electron + Jet Events, $m_T(e,\nu) < 45$ GeV/$c^2$

a) $E_T^e > 15$ GeV

| | MONTE CARLO | | | | | DATA |
|---|---|---|---|---|---|---|
| | Overlap + Conversions | W/Z | D.Y. J/$\Psi$ $\Upsilon$ | $b\bar{b}$ $c\bar{c}$ | TOTAL | |
| e + 0 jets | 3 ± 0.2 ± 0.5 | 26.9 ± 2 ±1.73 | 2.1 ± 0.4 ±0.72 | 1.8 ±0.4 ±0.45 | **33.8 ±2.1 ±2.0** | **34** |
| e + 1 jets | 5.5 ± 0.3 ± 1.0 | 5.3 ± 0.3 ±0.34 | 4.3 ±0.5 ±1.5 | 1.6 ±0.35 ±0.4 | **16.7 ±0.7 ±1.9** | **19** |
| e + ≥2 jets | 2.6 ± 0.3 ± 0.5 | 0.8 ± 0.2 ±0.06 | 1.1 ±0.3 ±0.38 | 2.2 ±0.45 ±0.55 | **6.7 ±0.6 ±0.7** | **7** |
| e + ≥1 jets | 8.1 ± 0.5 ± 1.5 | 6.1 ±0.4 ±0.4 | 5.4 ±0.6 ±1.9 | 3.8 ±0.6 ±0.95 | **23.4 ±0.9 ±2.7** | **26** |

b) 12 GeV ≤ $E_T^e$ ≤ 15 GeV

| | MONTE CARLO | | | | | DATA |
|---|---|---|---|---|---|---|
| | Overlap + Conversions | W/Z | D.Y. J/$\Psi$ $\Upsilon$ | $b\bar{b}$ $c\bar{c}$ | TOTAL | |
| e + ≥1 jets | 4.5 ± 0.2 ± 1.5 | 0.9 ±0.1 | 6.2 ±0.2 ±3.5 | 3.1 ±0.2 | **14.7 ±0.4 ±3.8** | **16** |

**Table 9: Expected TOP Event Rates for Isolated Electrons with $E_T^e$ > 15 GeV and accompanied by at least one jet.**

| | TOP MASS ( GeV/$c^2$ ) | | | | | |
|---|---|---|---|---|---|---|
| | **25** | **30** | **40** | **45** | **50** | **55** |
| $t\bar{b}$ | 3.3 ± 0.3 | 5.2 ± 0.5 | 6.2 ± 0.6 | 6.3 ± 0.6 | 6.0 ± 0.6 | 6.4 ± 0.6 |
| $t\bar{t}$ | 20.7 ± 0.9 | 14.1 ± 0.7 | 7.2 ± 0.5 | 3.2 ± 0.3 | 3.3 ± 0.3 | 2.0 ± 0.2 |
| **Total** | 24.0± 0.9 | 19.4± 0.9 | 13.4 ± 0.8 | 9.5 ± 0.7 | 9.3 ± 0.7 | 8.4 ± 0.6 |

**Table 10: Expected TOP Event Rates for Muon Pairs with $p_T^\mu$ > 3 GeV/c and Mass(μμ) > 6 GeV/$c^2$ .**

| | TOP MASS ( GeV/$c^2$ ) | | | |
|---|---|---|---|---|
| | **25** | **30** | **40** | **50** |
| $t\bar{b}$ | 3.3 ± 0.3 | 3.5 ± 0.3 | 3.0 ± 0.3 | 2.1 ± 0.2 |
| $t\bar{t}$ | 29 ± 1.3 | 13 ± 0.65 | 3.2 ± 0.2 | 1.3 ± 0.1 |
| **Total** | 32 ± 1.3 | 16.5 ± 0.7 | 6.2 ± 0.4 | 3.4 ± 0.2 |

## REFERENCES

[1] B. Adeva *et al.*, Phys. Rev. Lett. **50** (1983) 799.
W. Bartel *et al.*, Phys. Lett.,**132B** (1983) 241.
P. Avery *et al.*, Phys. Rev. Lett. **53** (1984) 1309.
A. Bean *et al.*, (CLEO Collaboration), CLNS 87/73.

[2] U. Amaldi *et al.*, Phys. Rev. **D36** (1987) 1385, and references therein.
G. Altarelli, talk presented at the Int. Europhysics Conf. on High Energy Physics, Uppsala, June 1987.
A. Sirlin, talk presented at the 1987 Int. Symp. on Lepton Photon Interactions at High Energy, Hamburg, July 1987.

[3] C. Albajar *et al.*, (UA1 Collaboration), Europhys. Lett. **1** (1986) 327.
R. Ansari *et al.*, (UA2 Collaboration), Phys. Lett. **B186** (1987) 440.

[4] H. Yoshida *et al.*, VENUS collaboration, Paper presented at the 1987 Int. Symp. on Lepton Photon Interactions at High Energy, Hamburg, July 1987.

[5] J. Ellis, J.S. Hagelin and S. Rudaz, Phys. Lett. **192B** (1987) 201;
V. Barger, T. Hau and D.V. Nanopoulos, Phys. Lett. **194B** (1987) 312;
I.I. Bigi and A.I. Sanda, Phys. Lett. **194B** (1987) 307;
L.L. Chau and W.Y. Keung, UC Davis preprint, UCD-87-02 (1987);
H. Harari and Y. Nir, SLAC-PUB-4341 (1987);
G. Altarelli and P.J. Franzini, CERN-TH.4745/87.

[6] H.J. Behrend et al., (CELLO Collaboration), Phys. Lett. **144B** (1984) 297.
See also S.Komamiya, Proc. Int. Symp. on Lepton Photon Interactions at High Energy, Kyoto, (1985) 612, and references therein.

[7] G. Arnison *et al.*, (UA1 Collaboration), Phys. Lett. **147B** (1984) 493.

[8] C. Albajar *et al.*, (UA1 Collaboration), "Study of Heavy Flavour Production in Events with a Muon Accompanied by Jet(s) at the CERN Proton-Antiproton Collider", CERN EP/87-189 submitted to Zeitschrift für Physik C.

[9] G. Arnison *et al.*, (UA1 Collaboration), Phys. Lett. **123B** (1983) 115.

[10] F. Paige and S.D. Protopopescu, ISAJET Monte Carlo, BNL 38034 (1986).

[11] C. Albajar *et al.*, (UA1 Collaboration), Phys. Lett. **186B** (1987) 237 and 247.
C. Albajar *et al.*, (UA1 Collaboration), "High Transverse Momentum J/Ψ Production at the CERN Proton-Antiproton Collider", CERN-EP/87-175, submitted to Phys. Lett. B.

[12] G. Arnison *et al.*, (UA1 Collaboration), Lett. Nuovo Cimento, **44** (1985) 1.
C. Albajar *et al.*, (UA1 Collaboration) "Studies of the W and $Z^0$ properties at the CERN Proton-Antiproton Collider", paper in preparation.

[13] T.H. Chang *et al.*, NIKHEF-H 81/34 (1981).
S. Gusken *et al.*, Phys.Lett. **155B** (1985) 185.
J.H. Kuhn *et al.*, Nucl.Phys. **B272** (1986) 560.
H.D. Tholl, Diploma Thesis, Aachen (1985).

[14] D.W. Duke and J.F. Owens, Phys. Rev. **D30** (1984) 49.

[15] M. Glück, E. Hoffman and E.Reya, Z. Phys. **C13** (1982) 119.

[16] E. Eichten *et al.*, Rev. Mod. Phys. **56** (1984) 579.

[17] A. Ali *et al.* , Nucl. Phys. **B292** (1987) 1;
B. Van Eijk, Ph.D. Thesis, University of Amsterdam (1987).

[18] C. Peterson *et al.*, Phys. Rev. **D27** (1983) 105.

[19] C. Albajar *et al.*, (UA1 Collaboration) , "Production of Low Transverse Energy Clusters in $p\bar{p}$ Collisions at $\sqrt{s}$ = 0.2 TeV - 0.9 TeV and their Interpretation in terms of QCD jets", paper in preparation.

[20] UA1 collaboration, Technical Notes, UA1-TN 86-26, 86-45 and 86-74 (unpublished).

[21] UA1 collaboration, Technical Note, UA1-TN 87-52 (unpublished).

[22] C. Albajar *et al.*,(UA1 Collaboration), Phys. Lett. **193B** (1987) 389

[23] UA1 Collaboration, Technical note, UA1-TN 87-75 (unpublished).

## FIGURE CAPTIONS

**Fig. 1** The expected number of events with one semi-leptonic decay of a top quark (e + μ) for an integrated luminosity equivalent to the total UA1 data sample of 700 $nb^{-1}$. The $p\bar{p} \rightarrow t\bar{t}X$, $W \rightarrow t\bar{b}$ and $Z \rightarrow t\bar{t}$ contributions are shown separately as dashed curves and the total as a solid curve. No selection criterion is applied to the charged lepton. The $p\bar{p} \rightarrow t\bar{t}$ X contribution is the full QCD prediction calculated using EUROJET. The $W \rightarrow t\bar{b}$ contribution is normalized to UA1 measurements. The dash-dotted curve shows the expected number of $t\bar{t}$ pairs yielding two Ws with one W decaying into lν and the other into two jets with $m_{jj} > 70$ GeV/$c^2$ .

**Fig. 2** The inclusive muon momentum spectrum, $d\sigma/dp_T^{\mu}$, versus $p_T^{\mu}$. The data are compared with Monte Carlo predictions including : $b\bar{b}$, $c\bar{c}$ , W, Z, Drell-Yan, J/ψ and ϒ. The top production for three different masses is shown ( $m_{top}$ = 25, 40 and 50 GeV/$c^2$) The data have been corrected for decay background and for acceptance, but not for muon momentum measurement errors.

**Fig. 3** The isolation variable ( $I = [(\Sigma E_T/3)^2 + (\Sigma p_T/2)^2]^{1/2}$ in a cone $\Delta R = 0.7$ around the muon ) distribution for the three sets of cuts described in the text:
a) $p_T^{\mu} > 10$ GeV/c, $E_T^{jet1} > 12$ GeV, $m_T^{\mu\nu} < 40$ GeV/$c^2$, no jet 2 requirement;
b) $p_T^{\mu} > 12$ GeV/c, $E_T^{jet1} > 15$ GeV, $m_T^{\mu\nu} < 40$ GeV/$c^2$, no jet 2 requirement;
c) $p_T^{\mu} > 12$ GeV/c, $E_T^{jet1} > 15$ GeV, $m_T^{\mu\nu} < 40$ GeV/$c^2$, $E_T^{jet2} > 7$ GeV.
The solid histogram is the Monte Carlo prediction of the background processes without top. The hatched area represents the contribution for a 30 GeV/$c^2$ mass top quark. The black points with error bars are the UA1 data.

**Fig. 4** Limit on the number of top quark events for the muon channel from rate alone. The 95% c.l. upper limit on the number of top events consistent with our measurement is indicated. The prediction for $W \rightarrow t\bar{b}$ plus $p\bar{p} \rightarrow t\bar{t}$ X is shown, as a function of top quark mass, by a shaded band which represents the total systematic error ( $\pm 1\ \sigma_{syst}$ ). The $t\bar{t}$ cross section is calculated using EUROJET. The $W \rightarrow t\bar{b}$ contribution (normalized to the UA1 measurements) is shown separately without errors.

**Fig. 5** Variables used to derive the top quark mass limit from the muon-jet data, shown for events with $p_T^{\mu} > 12$ GeV/c and $\geq 2$ jets.

a) The isolation variable, I. ( 104 events )
( $I = [(\Sigma E_T/3)^2 + (\Sigma p_T/2)^2]^{1/2}$ in a cone $\Delta R = 0.7$ around the muon )

b) The missing transverse energy: $E_T^{\nu}$. ( 17 events )

c) The transverse energy of jet 1: $E_T^{jet1}$. ( 10 events )

d) $|\cos(\theta^*)|$ for jet 2. ( 10 events )

b),c) and d) are given for events with $I < 2$, and a),c) and d) for events with $E_T^{jet1} > 15$ GeV. The points with error bars represent the data, the solid line all processes except top and the broken line the expected top contribution for a mass of 40 GeV/$c^2$.

**Fig. 6** Confidence level contours in the top quark cross section versus $m_{top}$ plane from muon information alone. The regions above the curves are excluded at the 90% and 95% confidence levels. The TRISTAN limit ( $m_{top} > 26$ GeV/$c^2$ ) is indicated. ($p\bar{p} \rightarrow t\bar{t}\,X$) refers to the EUROJET calculation.

**Fig. 7** Background to electron data. Number of events versus hadronic energy; a comparison between the prediction (histogram) for $\pi^{\pm}\pi^0$ overlaps and unseen conversions and the data (points with error bars), for electromagnetic clusters accompanied by at least one jet, with $m_T^{e\nu} < 45$ GeV/$c^2$.

**Fig. 8** Comparison between electron + $\geq 1$ jet events and Monte Carlo predictions for the non-top background.

a) the transverse energy of the electron, $E_T^e$,

b) the transverse energy of jet 1, $E_T^{jet1}$,

c) the difference in azimuthal angle between the electron and jet 1,

d) $\cos(\theta^*)$ for jet 2.

The points with error bars are the data, the solid line the Monte Carlo.

**Fig. 9** Limit on the number of top quark events for the electron channel from rate alone. The 95% c.l. upper limit on the number of top events consistent with our measurement is indicated. The prediction for $W \rightarrow t\bar{b}$ plus $p\bar{p} \rightarrow t\bar{t}\,X$ is shown, as a function of top quark mass, by a shaded band which represents the total experimental systematic errors ( $\pm 1\,\sigma$ ). The $t\bar{t}$ cross section is calculated using EUROJET. The $W \rightarrow t\bar{b}$ contribution (normalized to UA1 measurements) is shown separately without errors.

**Fig.10** Variables used for top quark mass limits from electron - jet data.
a) The missing transverse energy $E_T^{\nu}$, for events with at least one jet.
b) The jet multiplicity $N^{jet}$.
The points with error bars represent the data, the solid line all processes except top, the broken line the expected top contribution for a mass of 40 GeV/$c^2$.

**Fig.11** Confidence level contours in the top quark cross section versus $m_{top}$ plane from electron information alone. The regions above the curves are excluded at the 90% and 95% confidence levels respectively. The TRISTAN limit ( $m_{top} > 26$ GeV/$c^2$ ) is indicated. ($p\bar{p} \rightarrow t\bar{t}\,X$ ) refers to the EUROJET calculation.

**Fig.12** Confidence level contours in the top quark cross section versus $m_{top}$ plane from electron and muon information combined. The regions above the curves are excluded at the 90% and 95% confidence levels respectively. The TRISTAN limit ( $m_{top} > 26$ GeV/$c^2$ ) is indicated. ($p\bar{p} \rightarrow t\bar{t}\,X$ ) refers to the EUROJET calculation.

**Fig.13** Sensitivity of the mass limit to the ratio $K = \sigma(t\bar{t})/\sigma_o$, where $\sigma_o$ is the lowest order cross section calculation using EHLQ I structure functions and $Q^2 = m_{top}^2 + p_T^2$ (K=1). The choice of structure functions (DO1) and $Q^2$ scale ($Q^2 = \hat{s}$) giving the lowest predicted cross section is shown as a shaded curve. The EUROJET calculation corresponds to K = 1.5.

**Fig.14** Confidence level contours in the b' cross section versus $m_{b'}$ plane from electron and muon information combined. The regions above the curves are excluded at the 90% and 95% confidence levels respectively. The PETRA limit ( $m_{b'} > 22.7$ GeV/$c^2$ ) is indicated. ($p\bar{p} \rightarrow b'\bar{b}'X$ ) refers to the EUROJET calculation.

**Fig.15** Log-likelihood function used to place limits on the number of top quark candidates in dimuon events.

**Fig.16** Confidence level contours in the top quark cross section versus $m_{top}$ plane from muon pair information. The regions above the curves are excluded at the 90% and 95% confidence levels respectively. ($p\bar{p} \rightarrow t\bar{t}\,X$) refers to the EUROJET calculation.

**Fig.17** Mass plots for the muon channel. The mass M4 (muon–transverse neutrino–jet 1–jet 2 ) versus the mass M3 (muon–transverse neutrino–jet 2). On each projection of the scatter plot, the solid histogram shows the Monte Carlo prediction for the background processes without top. The dotted line histogram is the predicted shape for a top quark of mass 40 GeV/$c^2$, normalized to the total number of events in the data.

**Fig.18** Mass plots for the electron channel. The mass M4 (electron–transverse neutrino–jet 1–jet 2) versus the mass M3 (electron–transverse neutrino–jet 2). On each projection of the scatter plot, the solid histogram shows the Monte Carlo prediction for the background processes without top. The dotted line histogram is the predicted shape for a top quark of mass 40 GeV/$c^2$, normalized to the total number of events in the data.

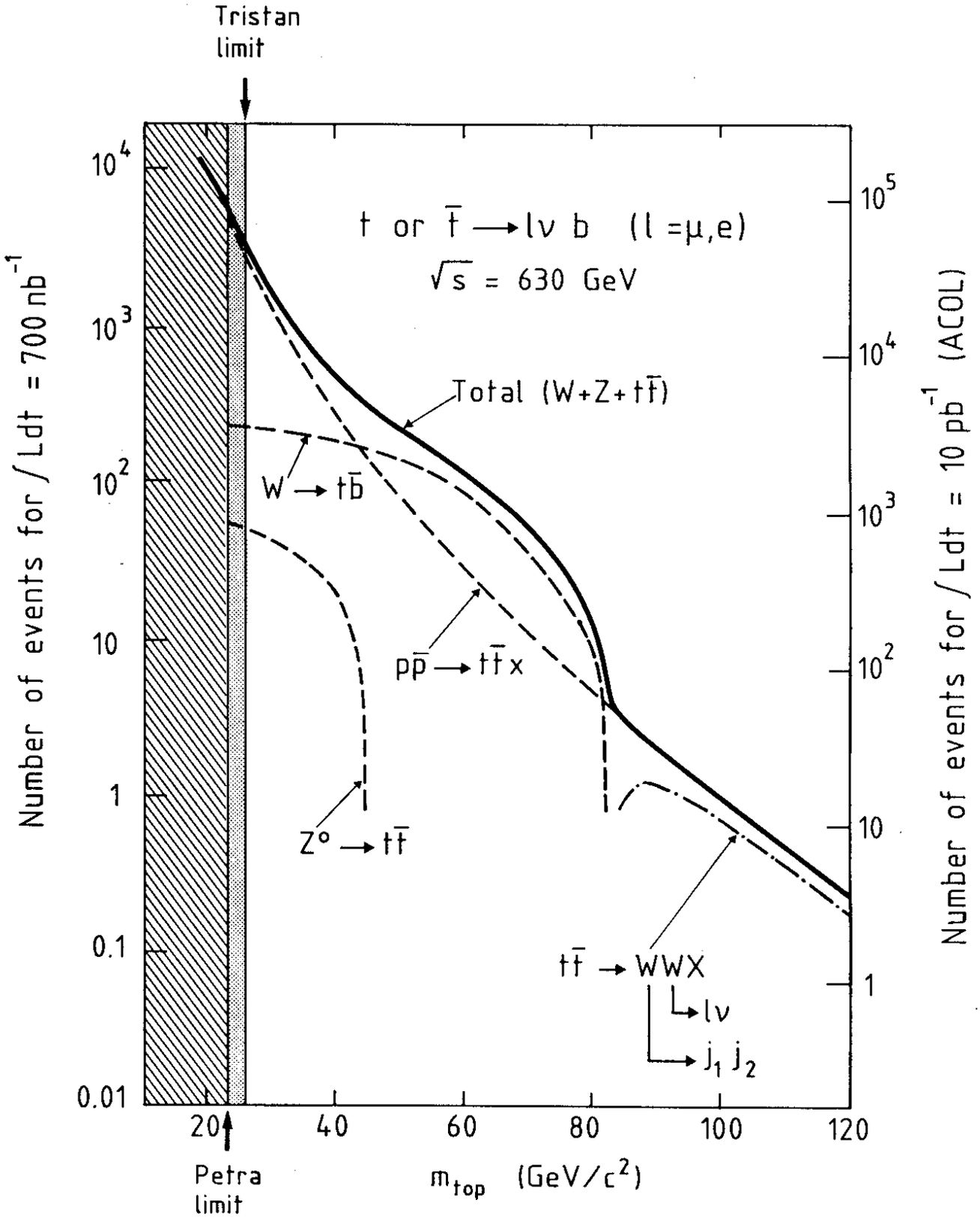
Tristan
limit
t or $\bar{t}$ → lν b (l = μ, e)
$\sqrt{s}$ = 630 GeV
Total (W+Z+$t\bar{t}$)
W → $t\bar{b}$
$p\bar{p}$ → $t\bar{t}$ x
Z° → $t\bar{t}$
$t\bar{t}$ → WWX
lν
$j_1$ $j_2$
Number of events for ∫Ldt = 700 nb$^{-1}$
Number of events for ∫Ldt = 10 pb$^{-1}$ (ACOL)
$m_{top}$ (GeV/$c^2$)
Petra
limit
10$^4$
10$^3$
10$^2$
10
1
0.1
0.01
10$^5$
10$^4$
10$^3$
10$^2$
10
1
20
40
60
80
100
120

**FIG. 1.**

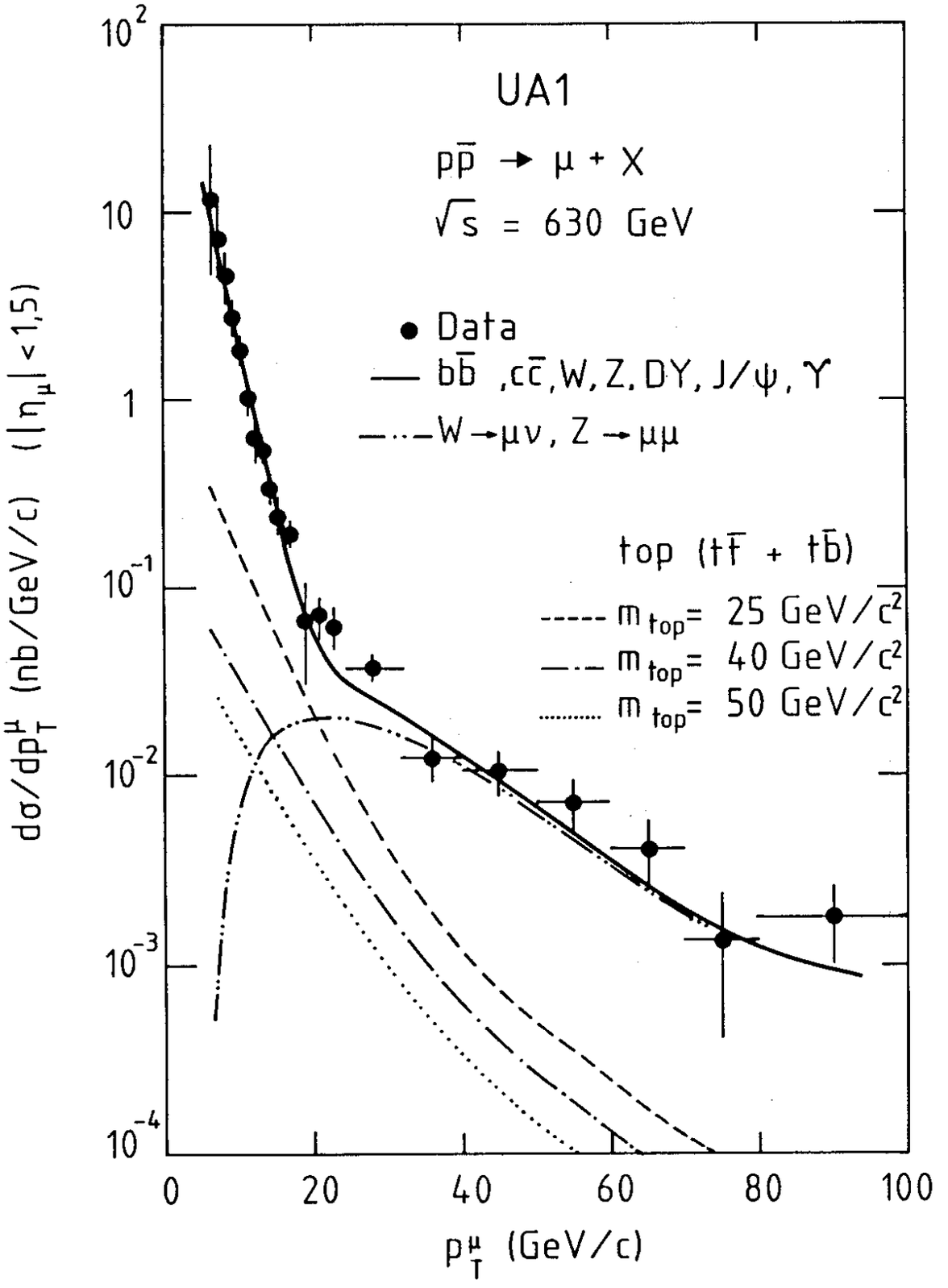
UA1
$p\bar{p} \rightarrow \mu + X$
$\sqrt{s}$ = 630 GeV
Data
$b\bar{b}$ , $c\bar{c}$, W, Z, DY, J/ψ, ϒ
$W \rightarrow \mu\nu$, $Z \rightarrow \mu\mu$
top ($t\bar{t}$ + $t\bar{b}$)
$m_{top}$= 25 GeV/$c^2$
$m_{top}$= 40 GeV/$c^2$
$m_{top}$= 50 GeV/$c^2$
$d\sigma/dp_T^\mu$ (nb/GeV/c) ($|\eta_\mu| < 1,5$)
$p_T^\mu$ (GeV/c)
$10^2$
10
1
$10^{-1}$
$10^{-2}$
$10^{-3}$
$10^{-4}$
0
20
40
60
80
100

**FIG. 2**

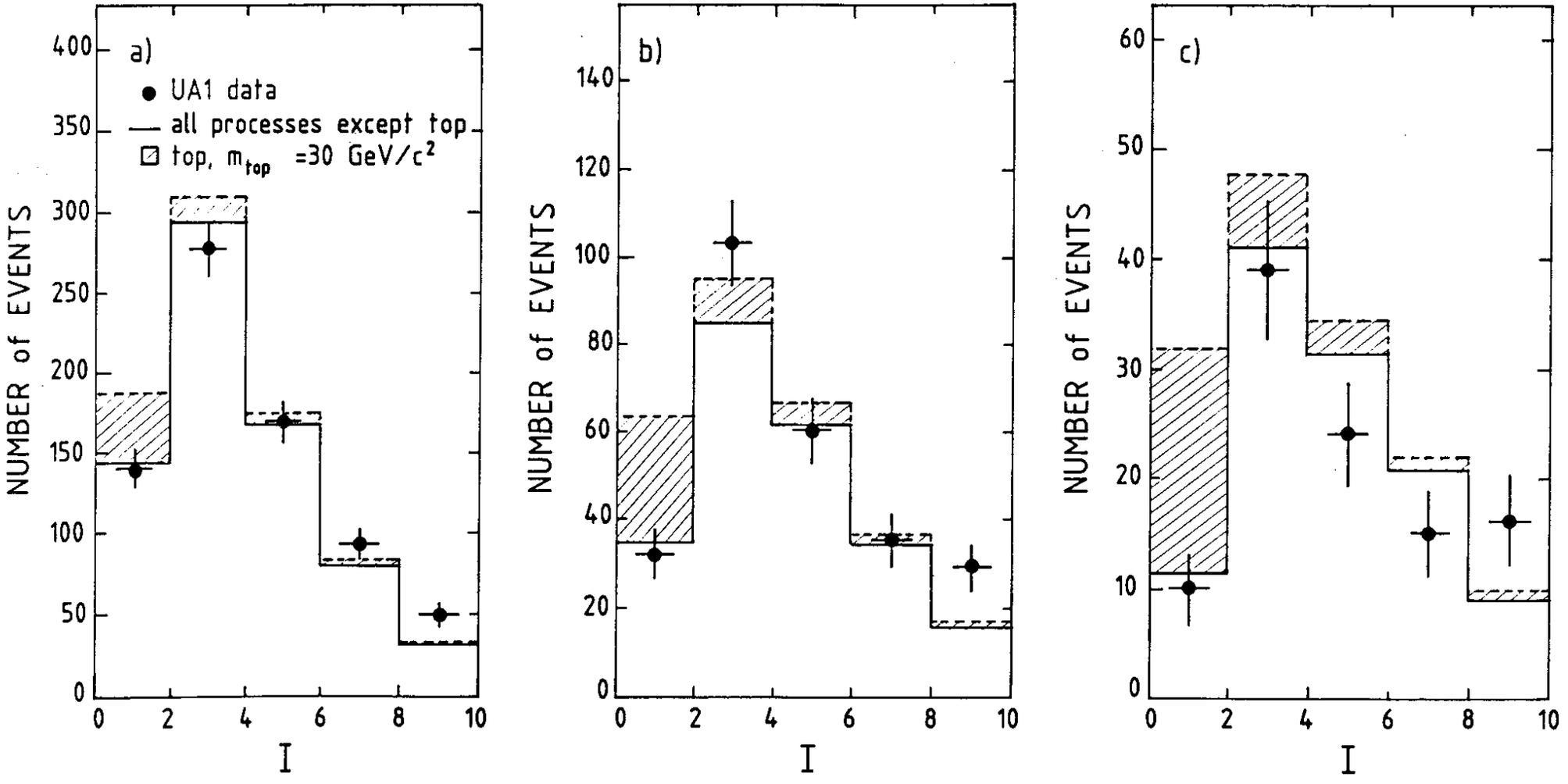
a)
UA1 data
all processes except top
top, $m_{top}$ =30 GeV/$c^2$
NUMBER of EVENTS
I
b)
NUMBER of EVENTS
I
c)
NUMBER of EVENTS
I

FIG. 3

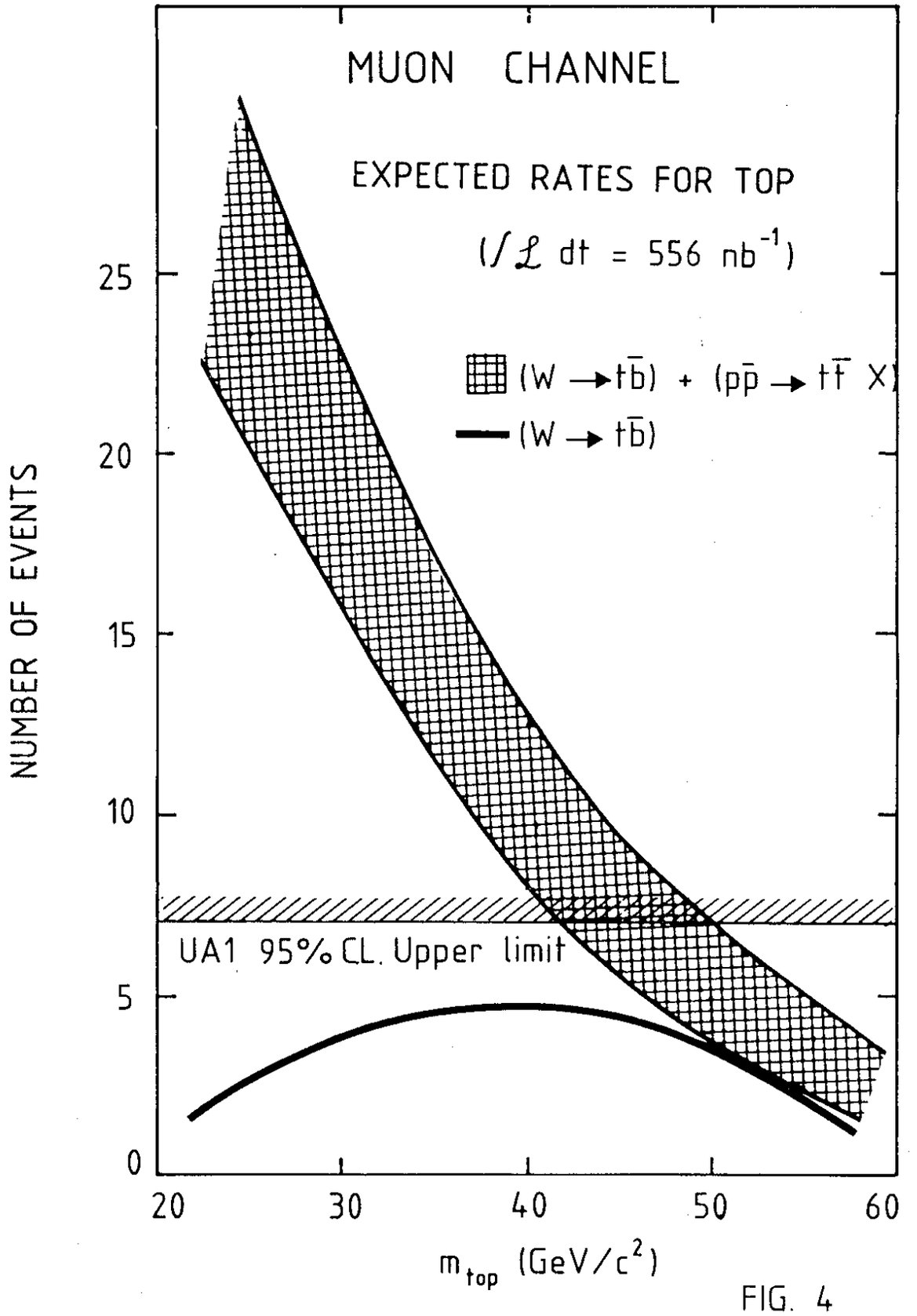
MUON CHANNEL
EXPECTED RATES FOR TOP
$(\int \mathcal{L}\, dt = 556\ nb^{-1})$
$(W \rightarrow t\bar{b}) + (p\bar{p} \rightarrow t\bar{t}\ X)$
$(W \rightarrow t\bar{b})$
UA1 95% CL. Upper limit
NUMBER OF EVENTS
0
5
10
15
20
25
20
30
40
50
60
$m_{top}$ (GeV/$c^2$)

FIG. 4

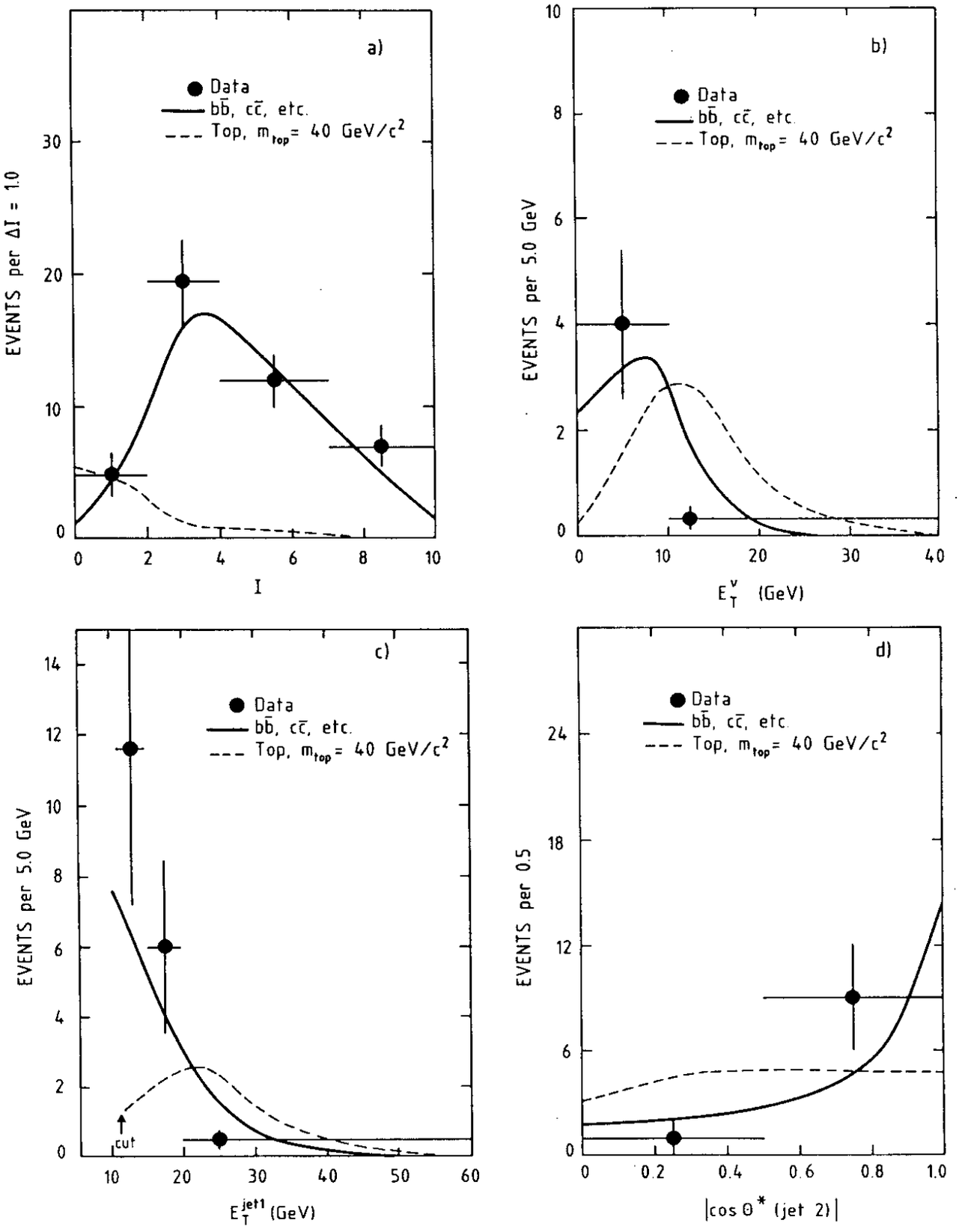
a)
Data
bb̄, cc̄, etc.
Top, m_top = 40 GeV/c²
EVENTS per ΔI = 1.0
I
b)
Data
bb̄, cc̄, etc.
Top, m_top = 40 GeV/c²
EVENTS per 5.0 GeV
E_T^ν (GeV)
c)
Data
bb̄, cc̄, etc.
Top, m_top = 40 GeV/c²
EVENTS per 5.0 GeV
cut
E_T^jet1 (GeV)
d)
Data
bb̄, cc̄, etc.
Top, m_top = 40 GeV/c²
EVENTS per 0.5
|cos Θ* (jet 2)|

FIG. 5

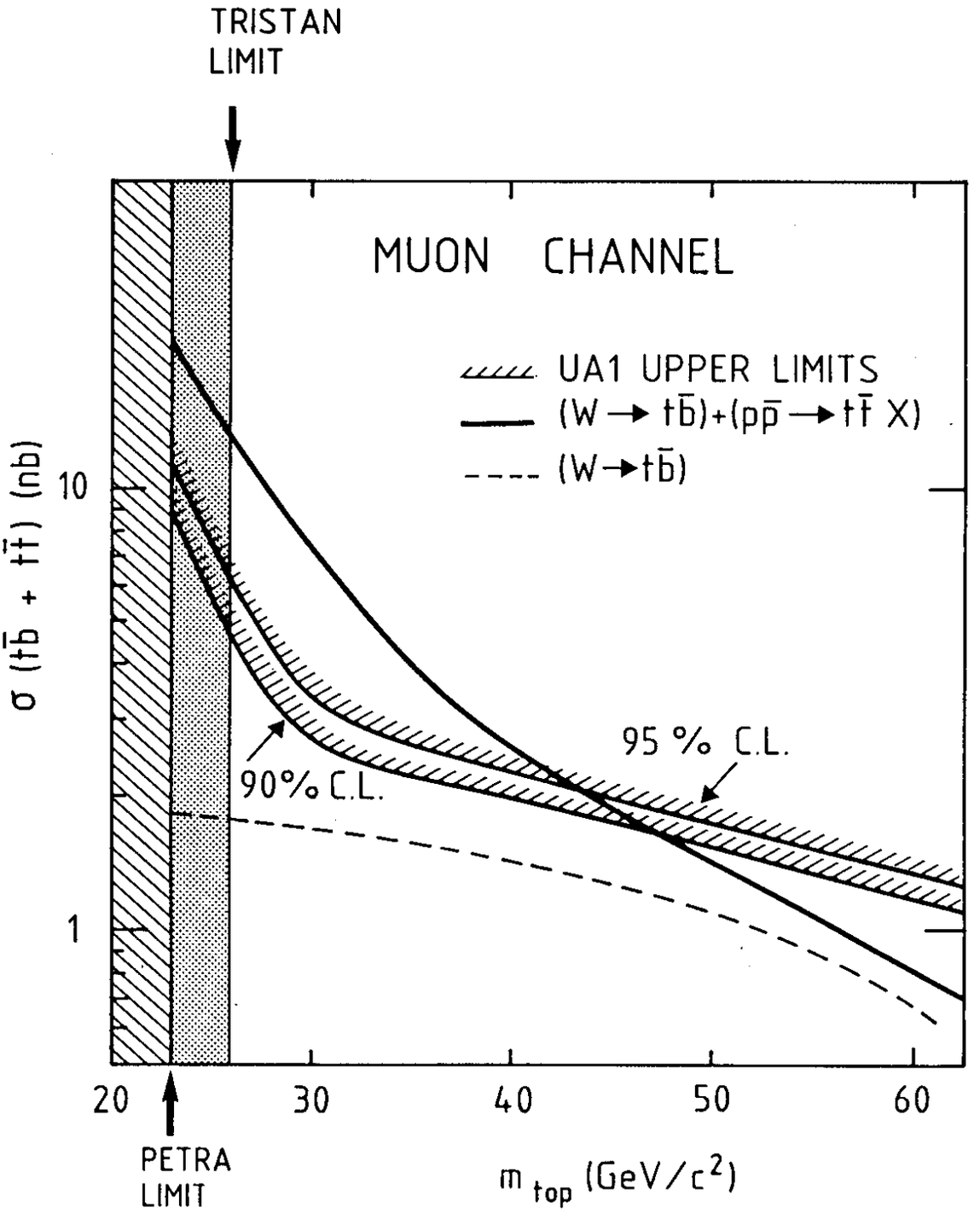
TRISTAN
LIMIT
MUON CHANNEL
UA1 UPPER LIMITS
(W → tb̄)+(pp̄ → tt̄ X)
(W → tb̄)
95 % C.L.
90% C.L.
σ (tb̄ + tt̄) (nb)
10
1
20
30
40
50
60
PETRA
LIMIT
m top (GeV/c²)

FIG. 6

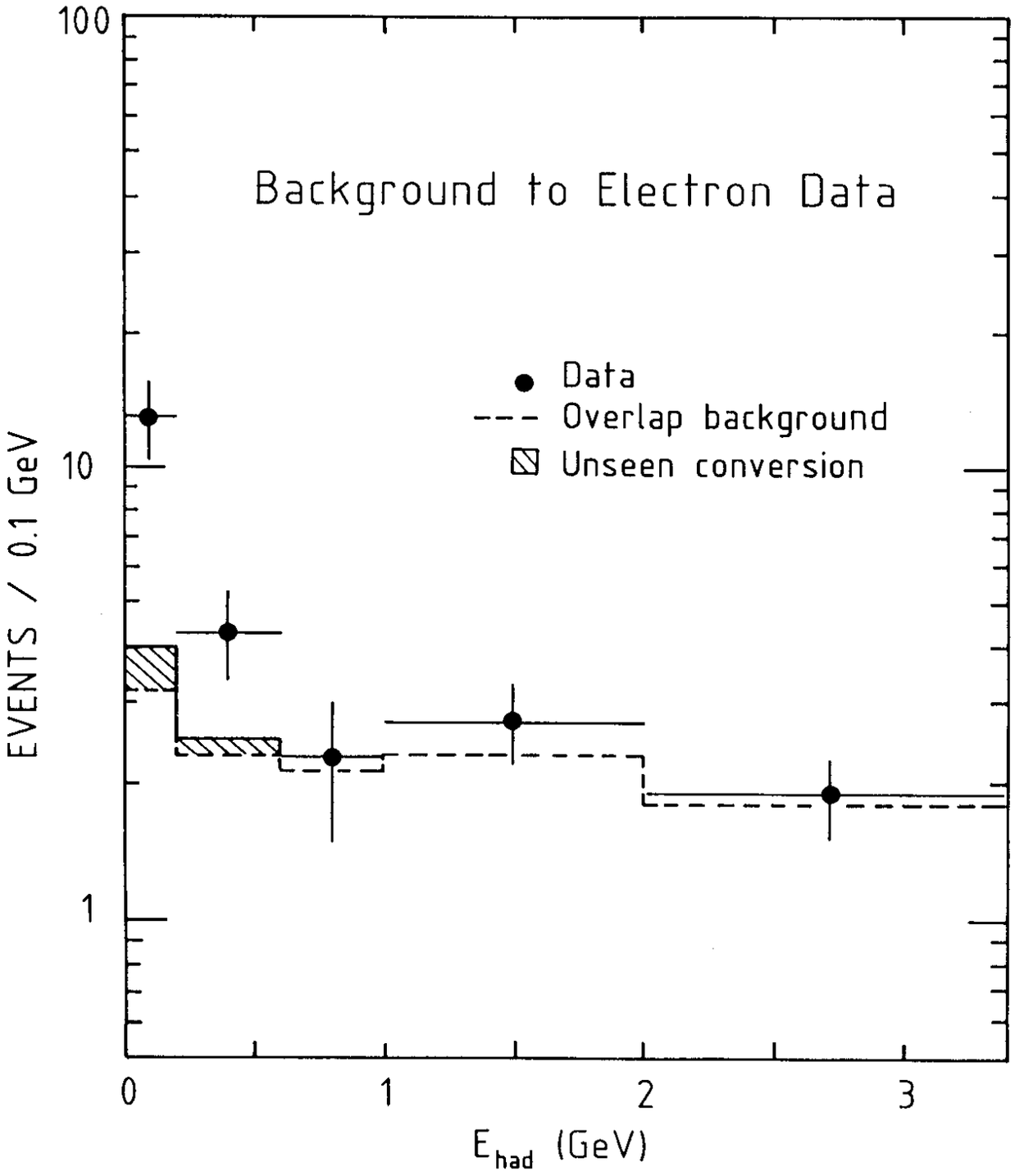
Background to Electron Data
Data
Overlap background
Unseen conversion
EVENTS / 0.1 GeV
100
10
1
0
1
2
3
E had (GeV)

FIG. 7

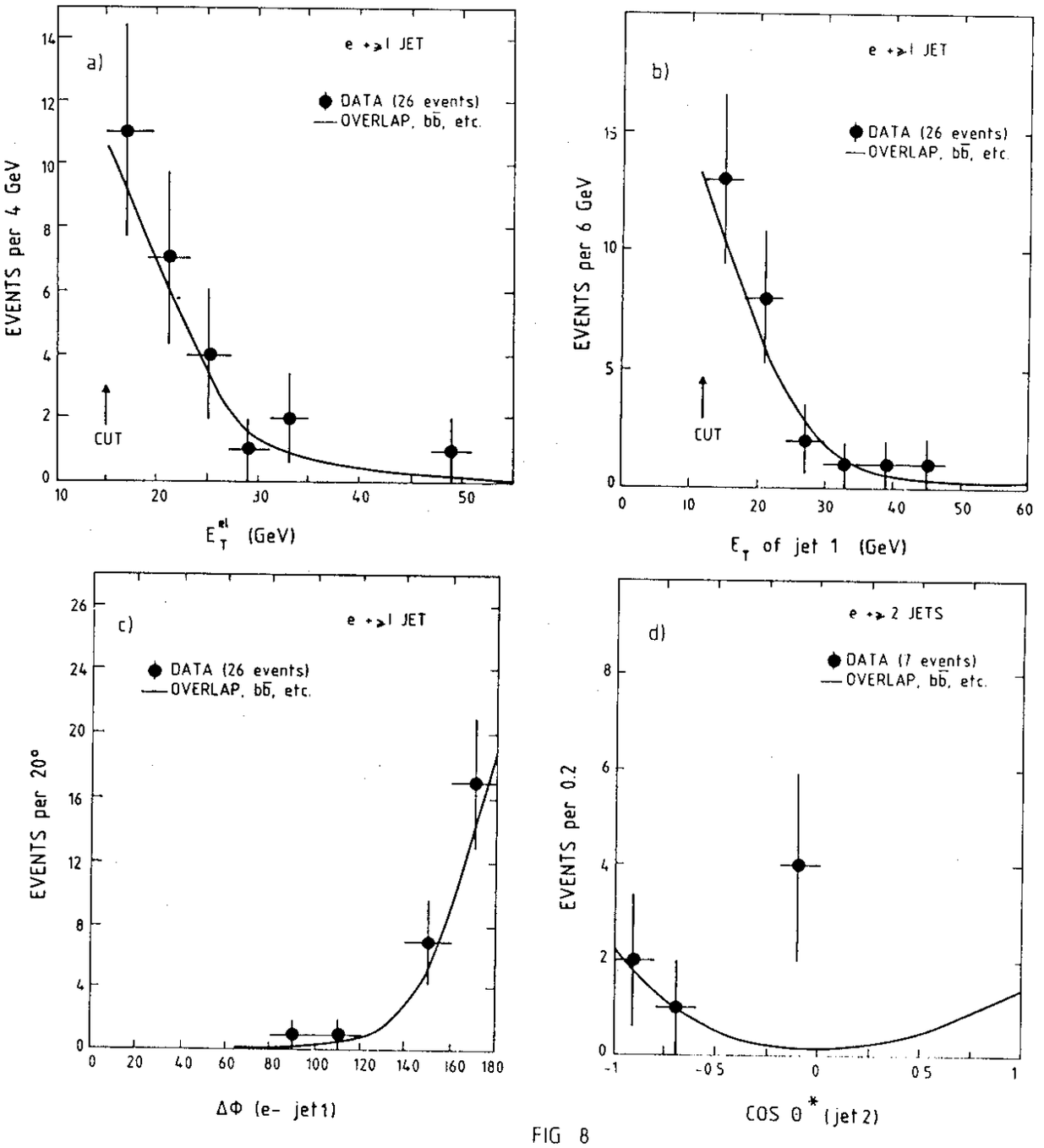
a)
e +≥1 JET
DATA (26 events)
OVERLAP, bb̄, etc.
CUT
EVENTS per 4 GeV
$E_T^{el}$ (GeV)
b)
e +≥1 JET
DATA (26 events)
OVERLAP, bb̄, etc.
CUT
EVENTS per 6 GeV
$E_T$ of jet 1 (GeV)
c)
e +≥1 JET
DATA (26 events)
OVERLAP, bb̄, etc.
EVENTS per 20°
ΔΦ (e- jet1)
d)
e +≥2 JETS
DATA (7 events)
OVERLAP, bb̄, etc.
EVENTS per 0.2
COS θ* (jet2)

FIG 8

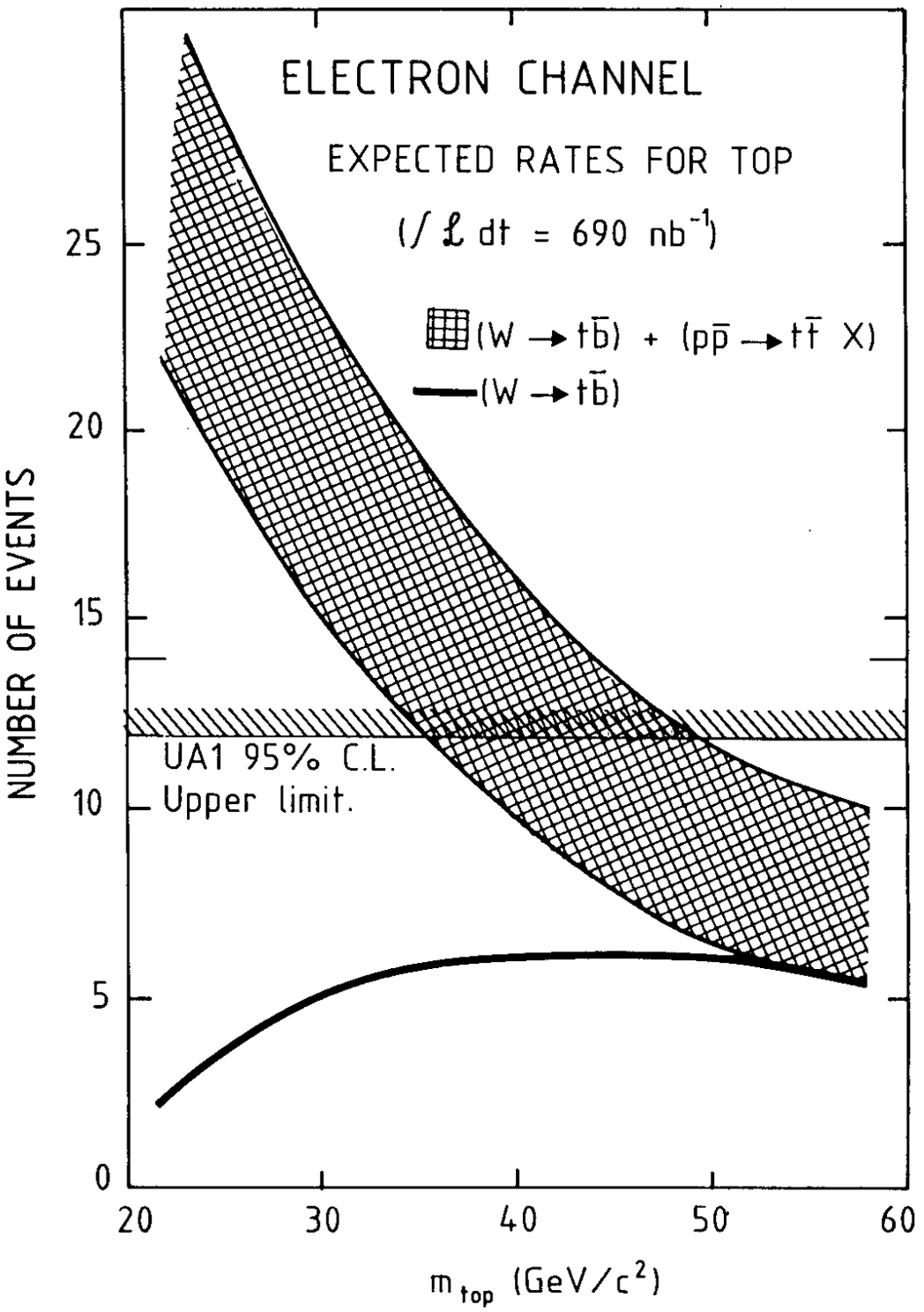
ELECTRON CHANNEL
EXPECTED RATES FOR TOP
(/ ℒ dt = 690 nb⁻¹)
(W → tb̄) + (pp̄ → tt̄ X)
(W → tb̄)
UA1 95% C.L.
Upper limit.
NUMBER OF EVENTS
0
5
10
15
20
25
20
30
40
50
60
m top (GeV/c²)

**FIG. 9**

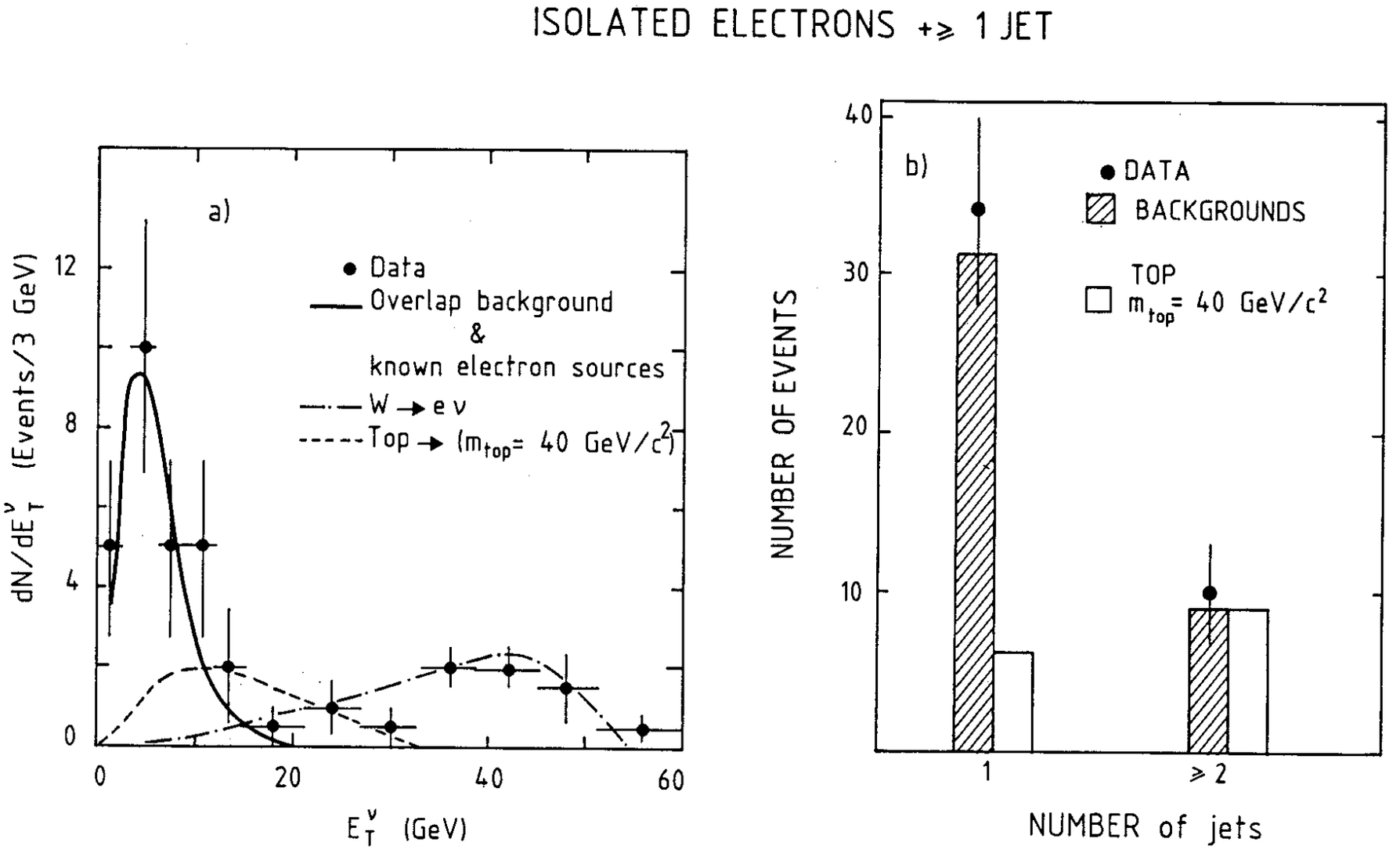
ISOLATED ELECTRONS +≥ 1 JET
a)
Data
Overlap background
&
known electron sources
W → e ν
Top → ($m_{top}$= 40 GeV/$c^2$)
$dN/dE_T^\nu$ (Events/3 GeV)
$E_T^\nu$ (GeV)
0
4
8
12
0
20
40
60
b)
DATA
BACKGROUNDS
TOP
$m_{top}$= 40 GeV/$c^2$
NUMBER OF EVENTS
NUMBER of jets
10
20
30
40
1
≥ 2

**FIG. 10**

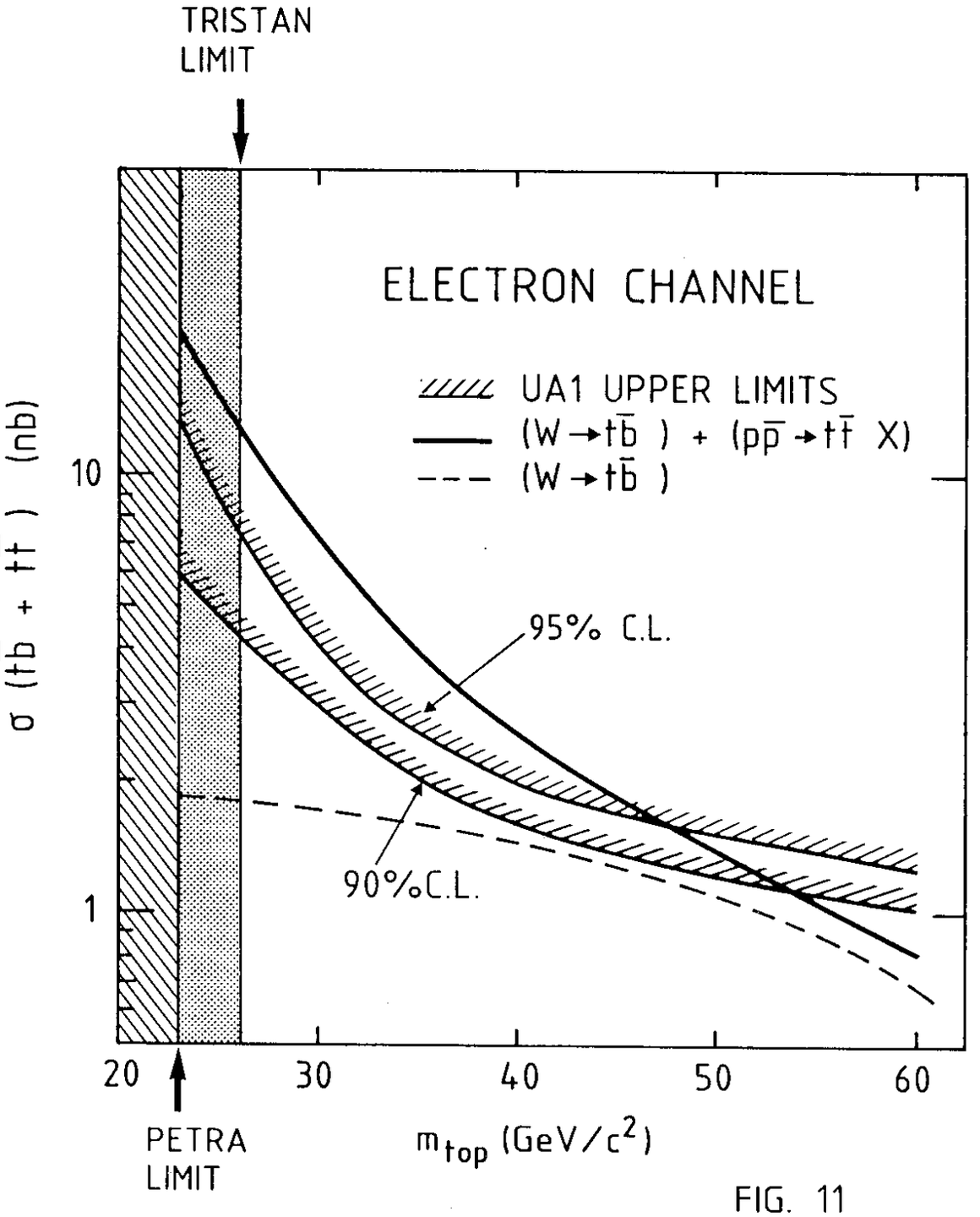
TRISTAN
LIMIT
ELECTRON CHANNEL
UA1 UPPER LIMITS
(W→tb̄ ) + (pp̄→tt̄ X)
(W→tb̄ )
95% C.L.
90%C.L.
σ (tb̄ + tt̄ ) (nb)
10
1
20
30
40
50
60
PETRA
LIMIT
m top (GeV/c²)

FIG. 11

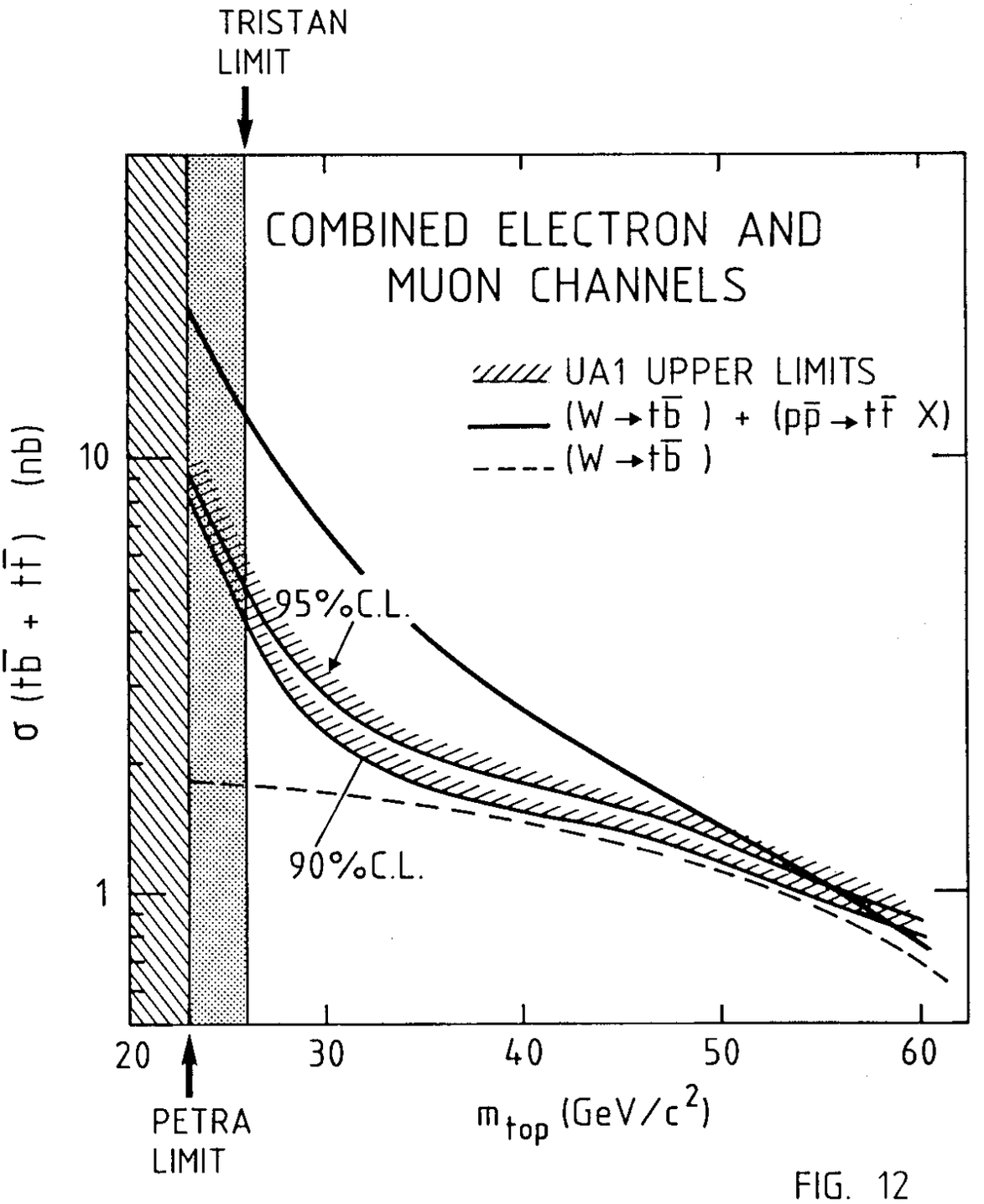
TRISTAN
LIMIT
COMBINED ELECTRON AND
MUON CHANNELS
UA1 UPPER LIMITS
(W → tb̄ ) + (pp̄ → tt̄ X)
(W → tb̄ )
95%C.L.
90%C.L.
σ (tb̄ + tt̄ ) (nb)
10
1
20
30
40
50
60
PETRA
LIMIT
m top (GeV/c²)

FIG. 12

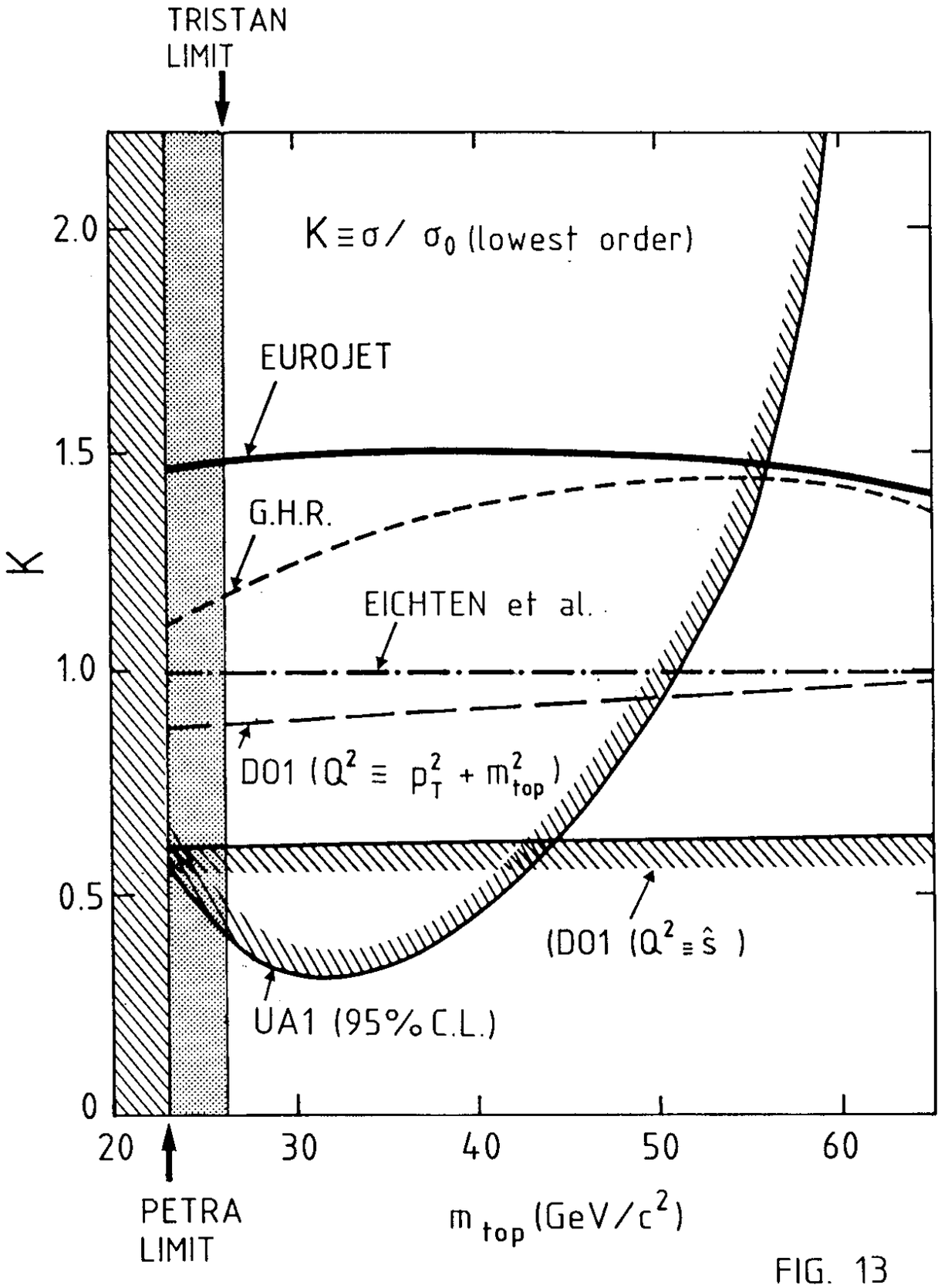
TRISTAN
LIMIT
$K \equiv \sigma / \sigma_0$ (lowest order)
EUROJET
G.H.R.
EICHTEN et al.
DO1 ($Q^2 \equiv p_T^2 + m_{top}^2$)
(DO1 ($Q^2 \equiv \hat{s}$)
UA1 (95% C.L.)
K
2.0
1.5
1.0
0.5
0
20
30
40
50
60
PETRA
LIMIT
$m_{top}$ (GeV/$c^2$)

FIG. 13

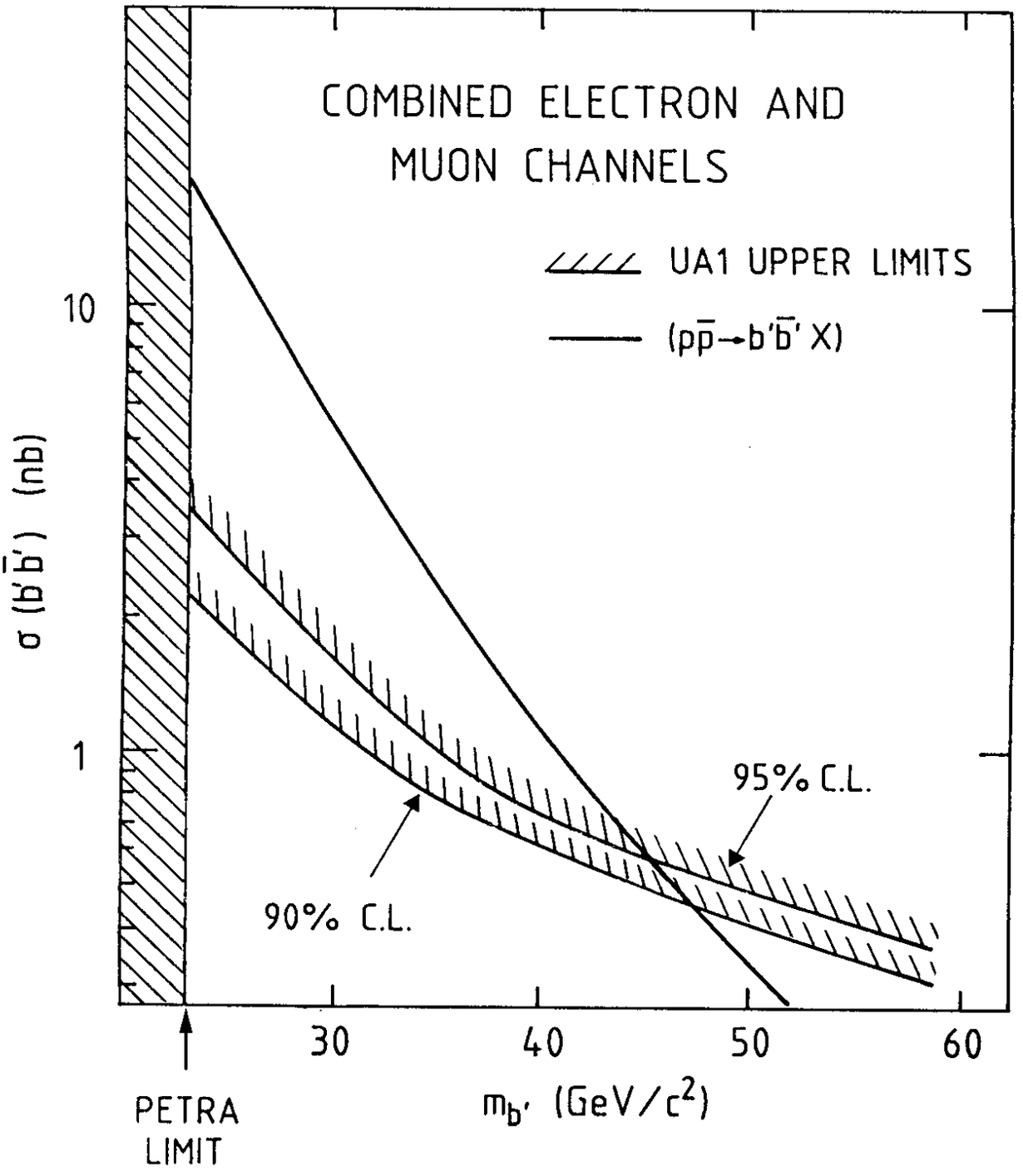
COMBINED ELECTRON AND
MUON CHANNELS
UA1 UPPER LIMITS
(pp̄→b'b̄' X)
95% C.L.
90% C.L.
10
1
σ (b'b̄') (nb)
30
40
50
60
PETRA
LIMIT
m_b' (GeV/c²)

FIG. 14

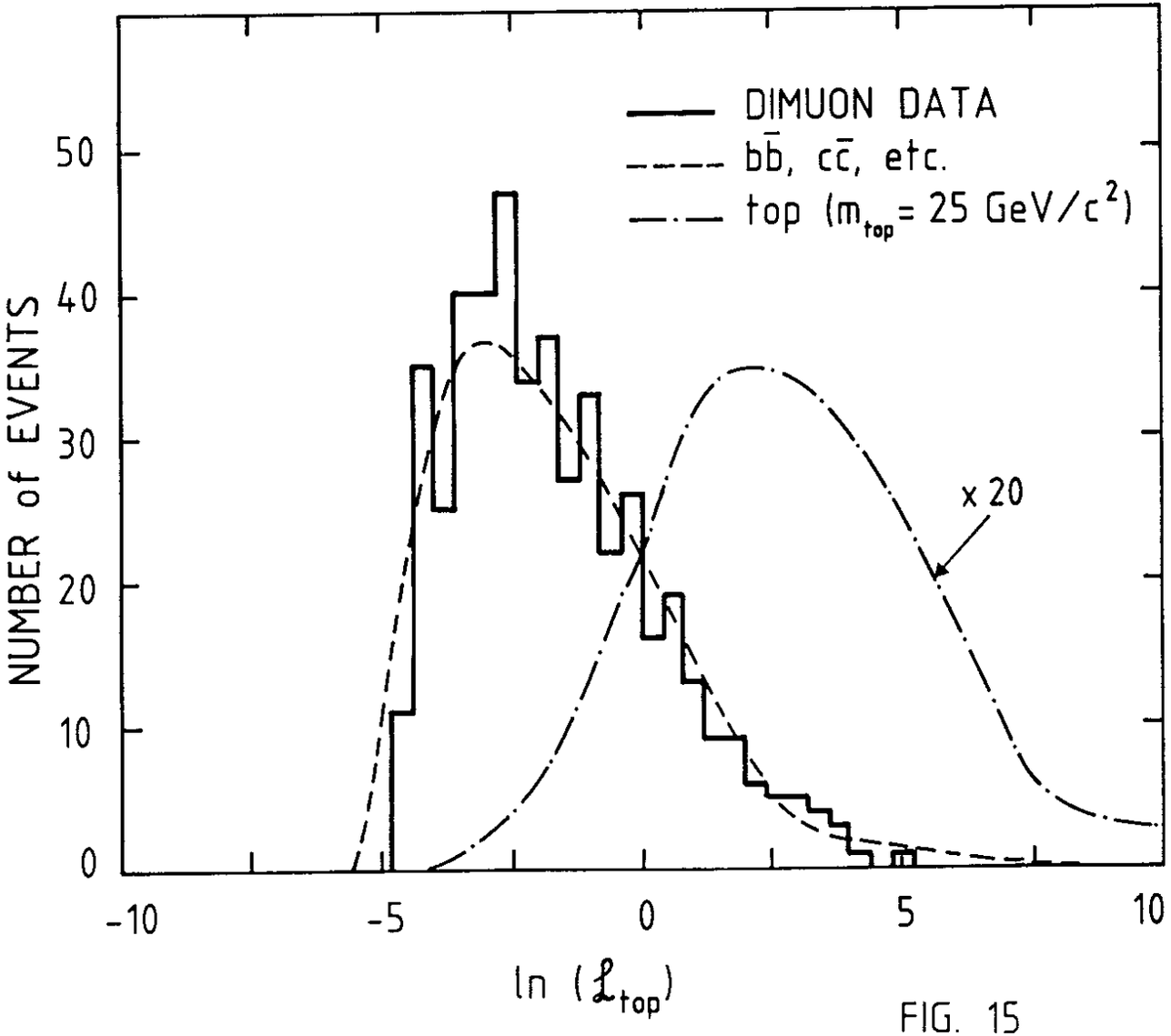
DIMUON DATA
$b\bar{b}$, $c\bar{c}$, etc.
top ($m_{top}$ = 25 GeV/$c^2$)
x 20
NUMBER of EVENTS
0
10
20
30
40
50
-10
-5
0
5
10
ln ($\mathcal{L}_{top}$)

FIG. 15

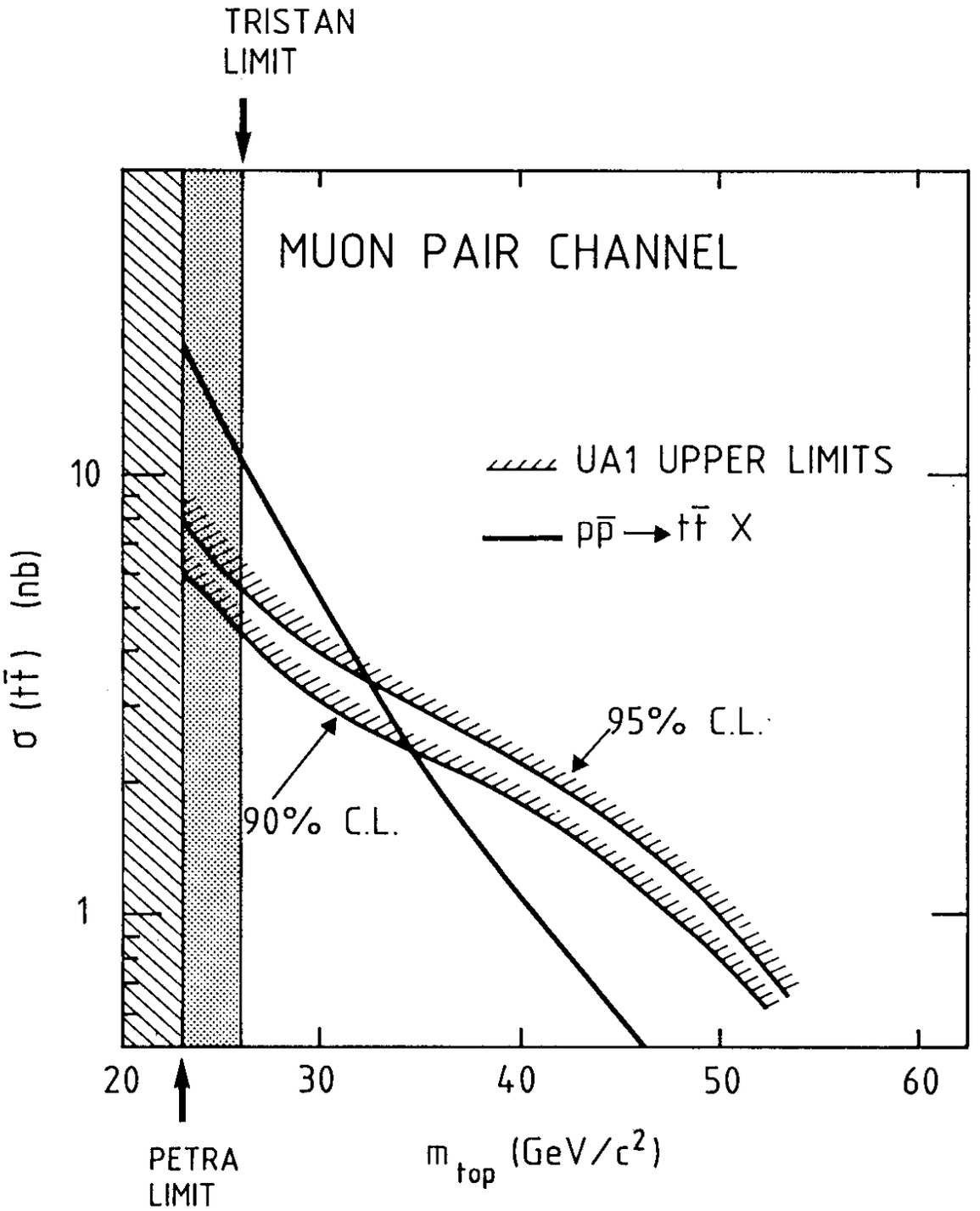
TRISTAN
LIMIT
MUON PAIR CHANNEL
UA1 UPPER LIMITS
$p\bar{p} \rightarrow t\bar{t}\ X$
95% C.L.
90% C.L.
10
1
$\sigma(t\bar{t})$ (nb)
20
30
40
50
60
PETRA
LIMIT
$m_{top}$ (GeV/$c^2$)

FIG. 16

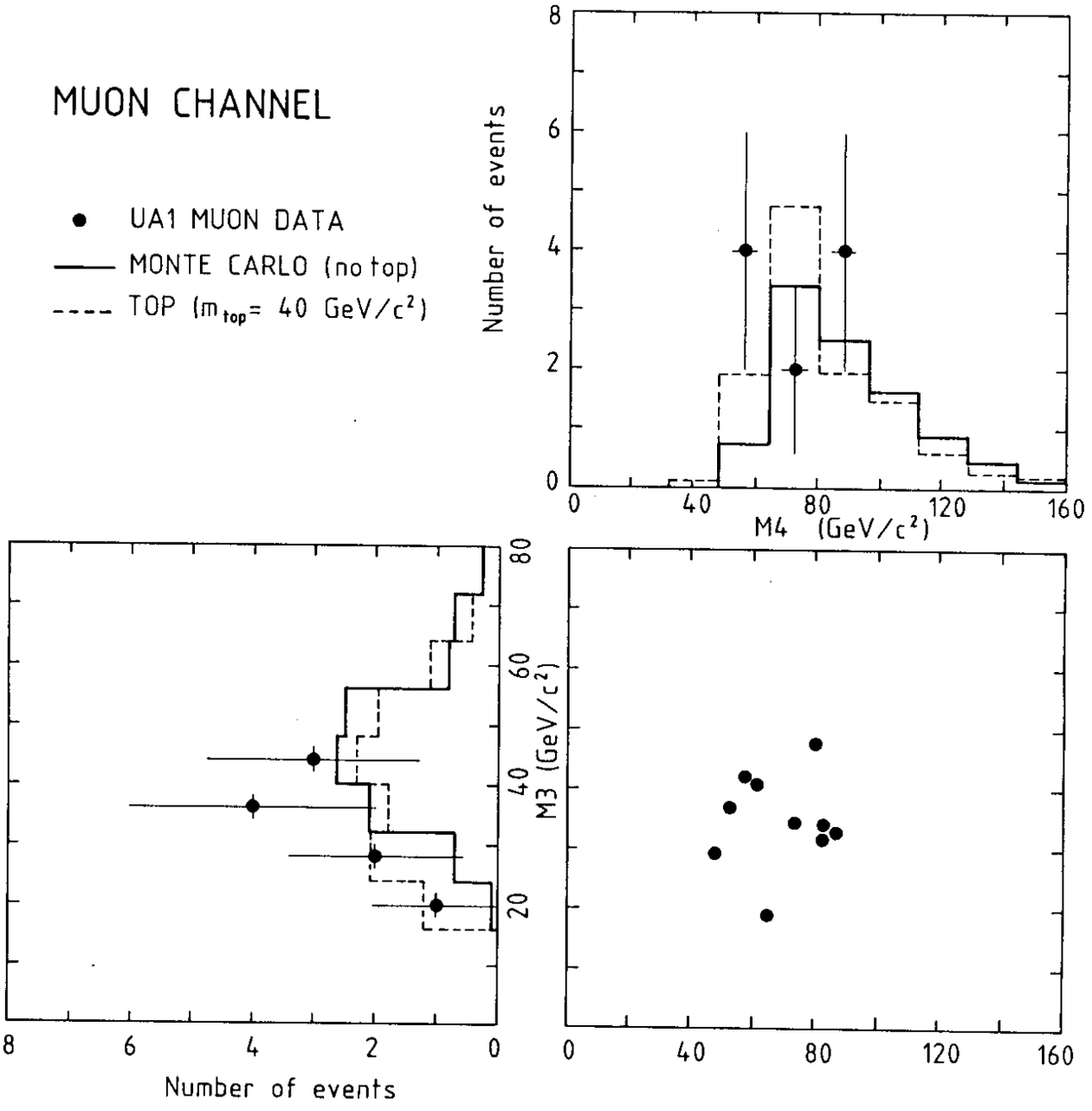
MUON CHANNEL
UA1 MUON DATA
MONTE CARLO (no top)
TOP ($m_{top}$= 40 GeV/$c^2$)
Number of events
M4 (GeV/$c^2$)
M3 (GeV/$c^2$)
Number of events

FIG. 17

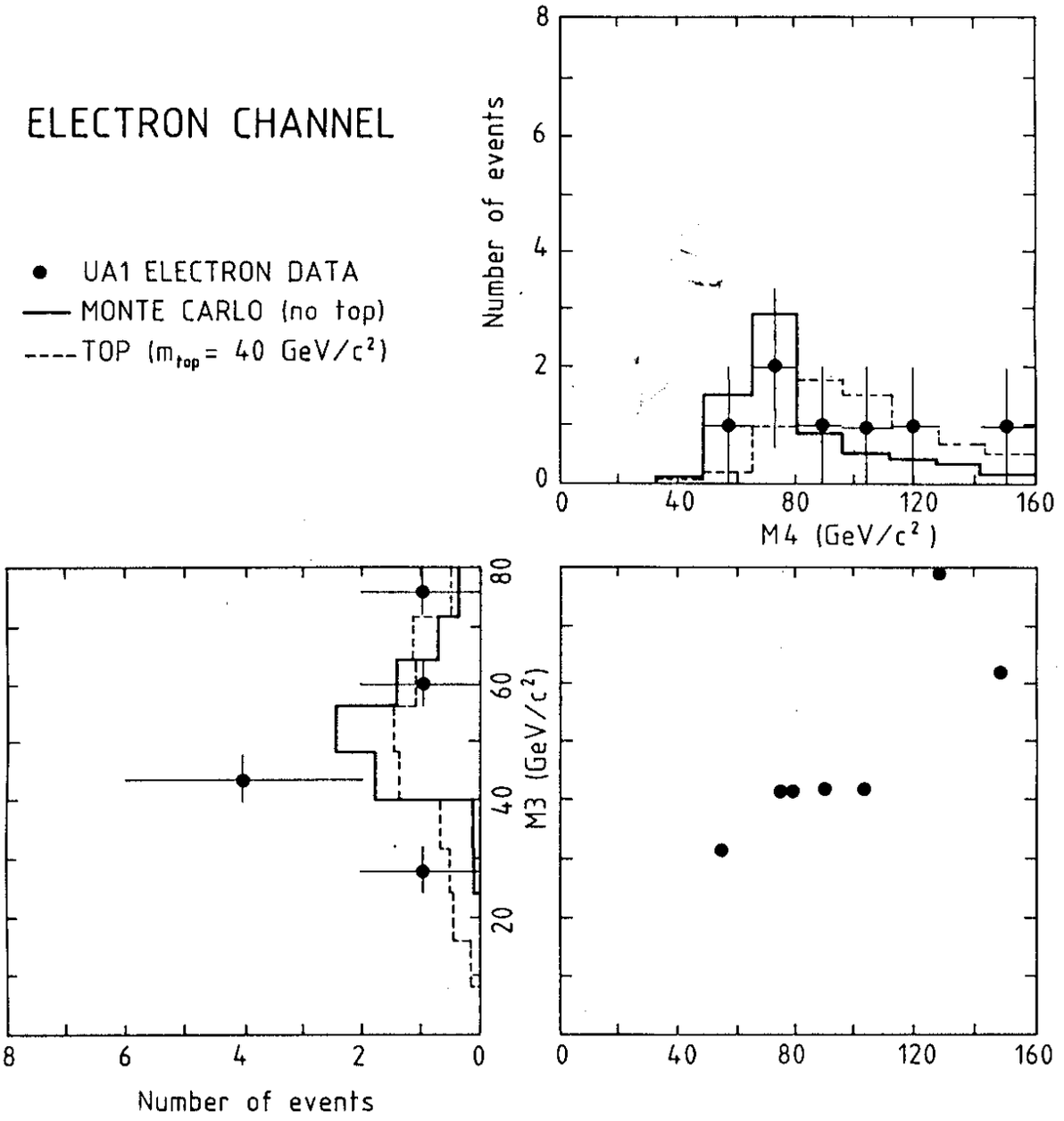
ELECTRON CHANNEL
UA1 ELECTRON DATA
MONTE CARLO (no top)
TOP ($m_{top}$ = 40 GeV/$c^2$)
Number of events
M4 (GeV/$c^2$)
M3 (GeV/$c^2$)
Number of events

FIG. 18